

copy 2

**MICHIGAN MEMORIAL PHOENIX PROJECT
PHOENIX MEMORIAL LABORATORY
THE UNIVERSITY OF MICHIGAN**

**ENERGETIC RECOIL ATOM REACTION MECHANISMS
PROGRESS REPORT NO. 1**

THIS WORK WAS SUPPORTED BY:

THE DEPARTMENT OF CHEMISTRY

THE MICHIGAN MEMORIAL PHOENIX PROJECT

THE UNITED STATES ATOMIC ENERGY COMMISSION
CONTRACT NO. AT(11-1)-912

THE UNIVERSITY
OF MICHIGAN
JAN 24 1973
PHOENIX
LIBRARY



T H E U N I V E R S I T Y O F M I C H I G A N
DEPARTMENT OF CHEMISTRY
MICHIGAN MEMORIAL-PHOENIX PROJECT

Progress Report No. 1

ENERGETIC RECOIL ATOM REACTION MECHANISMS

Adon A. Gordus, Principal Investigator

supported by

THE DEPARTMENT OF CHEMISTRY
THE MICHIGAN MEMORIAL-PHOENIX PROJECT

AND

THE U. S. ATOMIC ENERGY COMMISSION
CONTRACT NO. AT(11-1)-912

administered by

THE OFFICE OF RESEARCH ADMINISTRATION

ANN ARBOR

March, 1961

PREFACE

The following is a report of the work completed during the period June 1, 1960 to February 28, 1961. These studies were supported by the U. S. Atomic Energy Commission, Division of Research, Contract No. AT(11-1)-912, the Department of Chemistry of The University of Michigan, and the Michigan Memorial-Phoenix Projects 167 and 178.

TABLE OF CONTENTS

Preface -----	i
Table of Contents -----	ii
List of Tables -----	iii
List of Figures -----	iv
I. Introduction -----	1
II. Facilities -----	2
III. Gamma-Ray Recoil Energy Distributions -----	3
Random-Walk Equation -----	3
Cl ³⁵ (n,γ)Cl ³⁶ Process -----	10
IV. Activation by the (n,γ) Process -----	14
Calculation of Momentum Transfer -----	16
Applications -----	26
Experimentally Determined Failure to	
Bond-Rupture -----	29
V. Kinetic Theory of Hot Atom Reactions -----	36
VI. Br ⁸⁰ Activated by the (n,γ) Reaction -----	38
Effect of Molecular Additives on the	
Reaction with CH ₄ -----	46
VII. I ¹²⁸ Activated by the (n,γ) Reaction -----	51
A. Reaction with CH ₄ -----	51
1. Effect of Inert Gases -----	51
2. Effect of O ₂ , N ₂ , CF ₄ -----	68
3. Effect of CH ₂ F ₂ , C ₂ F ₆ -----	68
4. Effect of NO, CH ₃ I, n-C ₃ H ₇ I, CF ₃ I, C ₆ H ₆ --	71
VIII. Work in Progress -----	73
IX. Personnel, Publications and Talks -----	74
X. List of References -----	76

LIST OF TABLES

I.	Probability Distribution Function for Three Unequal Length Steps -----	6
II.	Various Cases for Four Unequal Length Steps -----	7
III.	Probability Distribution Function for Four Unequal Length Steps -----	8
IV.	Gamma-Ray Cascades from $\text{Cl}^{35}(\text{n},\gamma)\text{Cl}^{36}$ Process -----	11
V.	Net Gamma-Ray Recoil Energy Required for Carbon- Halogen Bond Rupture -----	27
VI.	Experimentally Determined Failure to Bond- Rupture -----	31
VII.	Percent Br^{80} Stabilized in Organic Combination in Various Gaseous Mixtures -----	40
VIII.	Percent I^{128} (and I^{131}) Stabilized in Organic Combination in Various Gaseous Mixtures Contain- ing CH_4 and Inert Gases -----	52
IX.	Percent I^{128} Stabilized in Organic Combination in Various Mixtures Containing CH_4 and a Molecular Additive -----	63
X.	Percent I^{128} Stabilized in Organic Combination in Various Gaseous Mixtures of an Iodide and an Additive -----	67

LIST OF FIGURES

1.	Summed Probability Distribution for $\text{Cl}^{35}(\text{n},\gamma)\text{Cl}^{36}$ Gamma-Ray Energies -----	12
2.	Summed Probability for $\text{Cl}^{35}(\text{n},\gamma)\text{Cl}^{36}$ Gamma-Ray Energies -----	13
3.	Schematic Representation of Pseudo-Polyatomic Molecule -----	17
4.	General Spatial Coordinates for Pseudo-Polyatomic Molecule -----	20
5.	Resolution of Q_v Momentum Vector -----	23
6.	Br^{80} Failure to Bond-Rupture as a Function of Required Net Gamma Recoil Energy -----	34
7.	I^{128} Failure to Bond-Rupture as a Function of Required Net Gamma Recoil Energy -----	35
8.	Effect of Inert-Gas Moderators on the Reaction of CH_4 with Br^{80} Activated by the (n,γ) Process ----	44
9.	Effect of Molecular Moderators on the Reaction of CH_4 with Br^{80} Activated by the (n,γ) Process ----	45
10.	Plot Corresponding to Eq. 32 for the Br^{80} in Organic Combination -----	49
11.	Reactor-Radiation Induced Pickup of I^{131} in CH_4 -inert Gas Mixtures Containing CH_3I and I_2 -131 --	54
12.	Percent I^{128} as Organic Activity in CH_4 -Inert Gas Mixtures Containing CH_3I and I_2 -----	56
13.	Plot Corresponding to Eq. 32 for I^{128} in Organic Combination -----	59
14.	Effect of Xenon in Inhibiting the Reaction: $\text{I}^+(\text{}^1\text{D}_2) + \text{CH}_4 \rightarrow \text{CH}_3\text{I}^+ + \text{H}$ -----	60
15.	Effect of O_2 , N_2 , and CF_4 on the Reaction of I^{128} with CH_4 -----	69
16.	Effect of CH_2F_2 and C_2F_6 on the Reaction of I^{128} with CH_4 -----	70
17.	Effect of NO , CH_3I , CF_3I , C_6H_6 , and $\text{n-C}_3\text{H}_7\text{I}$ on the Reaction of I^{128} with CH_4 -----	72

I. INTRODUCTION

Our studies have been concerned principally with investigations of the chemical effects of nuclear transformations. The theoretical approach (Sections III and IV) has, to date, been limited to investigations of primary activation processes. The experimental studies (Sections VI and VII) have been aimed at studying the initial activation processes as well as hot-atom reaction mechanisms.

As a result of these studies it has been possible, in a number of instances, to obtain information which is of general applicability and occasionally would appear to be unrelated to the studies which have been undertaken. For example, the solution to the random-walk equation (Section III) is completely general, the calculation concerning the momentum-transfer required for bond-rupture (Section IV) is not limited to (n,γ) processes but is valid for any case of a randomly directed momentum impulse. Investigations of the effects of molecular additives on the (n,γ) activated reaction of I^{128} with CH_4 (Section VII) have yielded information concerning ion-molecule reactions and an approximate value for the ionization potential of C_2F_6 .

As a result of these studies we have been able to gain a greater understanding of high-energy and ionic reaction mechanisms. This understanding is far from complete; however, a number of important aspects concerning activated halogen atom/ion reactions have been explained.

II. FACILITIES

Michigan Reactor

All samples were irradiated in The University of Michigan-Ford Nuclear Reactor which is located in the Phoenix Memorial Laboratory on the North Campus of the University. This reactor is of a swimming pool design and is operated at a level of one megawatt. Samples are sent into the reactor via a pneumatic tube system. The thermal neutron flux under these conditions is about 2×10^{12} n-cm⁻²-sec⁻¹. The accompanying gamma-radiation flux is about 8000 roentgens per minute.

Phoenix Laboratory

Irradiated samples are prepared for analysis in a laboratory room in the Phoenix building. This room, which is used exclusively by our group, contains a six-foot "Oak Ridge-type" hood, and the usual laboratory facilities. To date, this area has proven adequate for our purposes.

Counting of the radioactivity is done in another room which is shared with others working in the Phoenix building.

In a few instances, it was necessary to analyse samples containing both I¹²⁸ (25 min.) and Cl³⁸ (37.5 min.) activity. Such analyses were performed on the 100-channel analyser which is under the supervision of Professor W. W. Meinke.

Chemistry Building

This group has been assigned the use of one small laboratory in the Chemistry building to be used for experimental studies involving isotopes. We are using this room for our studies involving the Br^{80m}(I.T.)Br⁸⁰ (4.5 hr.) reaction. For these experiments, liquid bromine is irradiated in the Ford Reactor and then transported to this room in the Chemistry building.

Non-radioactive sample preparations are performed in one of two other rooms in the Chemistry building where laboratory space has been made available.

III. GAMMA-RAY RECOIL ENERGY DISTRIBUTIONS

Random-Walk Equation

A closed general solution of the probability distribution function for three-dimensional random-walk processes has been derived. This derivation has appeared¹ in the February, 1961, issue of the Journal of Chemical Physics. Presented in the paper are the specific solutions for $n = 2, 3$, and 4 unequal-length steps.

The probability distribution function, $W_n(R)$, was shown to be:

$$W_n(R) = \frac{1}{2^{n+2} \pi R(n-2)! \prod_{i=1}^n l_i} \sum_{j=1}^{2^{n-1}} (M_j^{n-3} |M_j| - N_j^{n-3} |N_j|) \quad (1)$$

where l_i is the magnitude of the i 'th step and

1. both M_j and N_j are algebraic sums consisting of $(n+1)$ terms of R, l_1, l_2, \dots, l_n ;
2. there are a total of 2^{n-1} different M_j and 2^{n-1} different N_j terms;
3. the first quantity in each M_j or N_j terms is always positive;
4. the total number of negative signs in each M_j term is an odd number, $[1, 3, 5, \dots, (n-1)_e \text{ or } (n)_o]$;
5. the total number of negative signs in each N_j term is an even number, $[0, 2, 4, \dots, (n)_e \text{ or } (n-1)_o]$, where e and o represent n equal to an even or odd number, respectively.

The probability distribution is

$$d P_n(R)/dR = 4\pi R^2 W_n(R) \quad (2)$$

The probability that the total displacement is between 0 and R as a result of n random vector displacements is,

$$P_n(R) = \int_0^R 4\pi R^2 W_n(R) dR \quad (3)$$

Complete solutions for $W_2(R)$, $W_3(R)$, and $W_4(R)$ are given below. It should be noted that the signs and magnitudes of the M_j and N_j terms vary as a result of variations in R and as a result of these variations $W_n(R)$ is a piecewise continuous curve with respect to R . Consequently, $W_n(R)$, and thus $dP_n(R)/dR$ and $P_n(R)$ must be evaluated in segments.

Two Random Steps

For two random-length vectors, $\ell_1 = A$ and $\ell_2 = B$ where $A > B$, the solutions are trivial. There are $2^{2-1} = 2M_j$ and $2N_j$ terms. They are $M_1 = R-A+B$, $M_2 = R+A-B$, $N_1 = R+A+B$, $N_2 = R-A-B$. $W_2(R) = 0$ in the range $0 < R < (A-B)$ and $= 1/(8\pi RAB)$ in the range $(A-B) < R < (A+B)$.

Three Random Steps

For the process involving three random steps there exist two possible cases. Assuming $(\ell_1 = A) > (\ell_2 = B) > (\ell_3 = C)$, then these two cases are: 1. where $A > (B+C)$, or 2. where $A < (B+C)$. The four M_j and N_j terms are:

M_j		N_j
$M_1 = R+A+B-C$		$N_1 = R+A+B+C$
$M_2 = R+A-B+C$		$N_2 = R+A-B-C$
$M_3 = R-A+B+C$		$N_3 = R-A+B-C$
$M_4 = R-A-B-C$		$N_4 = R-A-B+C$

As an illustration, let us consider the calculation of $W_3(R)$ in the range $(A+B-C) \rightarrow (A+B+C)$, the solution being valid for both cases (1) and (2).

$$\begin{aligned}
 W_3(R) &= \frac{1}{32\pi RABC} \sum_{j=1}^{j=4} (|M_j| - |N_j|) \\
 &= \frac{M_1 + M_2 + M_3 - M_4 - N_1 - N_2 - N_3 - N_4}{32\pi RABC} \\
 &= \frac{-R + A + B + C}{16\pi RABC}
 \end{aligned}$$

The calculated values of $W_3(R)$ for all four ranges for each case are given in Table I.

Four Random Steps

For the process involving four random steps there exist eight M_j and eight N_j terms. Calling $\ell_1 = A$, $\ell_2 = B$, $\ell_3 = C$, and $\ell_4 = D$, and assigning $A > B > C > D$, there exist 14 different complete solutions depending on the particular numerical values for A , B , C , and D . These 14 cases are listed in Table II.

For each of these cases the range of $W_4(R)$ is divided into eight segments. In many instances, certain solutions of $W_4(R)$ are common to more than one of the above cases. The complete solutions of $W_4(R)$ for all 14 possible cases are given in Table III.

Table I. Probability distribution for
three unequal length steps.

R-range		Applicability ^a	$W_3(R)$
0	$\rightarrow (A-B-C)$	1	0
0	$\rightarrow (-A+B+C)$	2	$\frac{1}{8\pi ABC}$
$(A-B-C)$	$\rightarrow (A-B+C)$	1	$\frac{R-A+B+C}{16\pi RABC}$
$(-A+B+C)$	$\rightarrow (A-B+C)$	2	
$(A-B+C)$	$\rightarrow (A+B-C)$	1 or 2	$\frac{1}{8\pi RAB}$
$(A+B-C)$	$\rightarrow (A+B+C)$	1 or 2	$\frac{-R+A+B+C}{16\pi RABC}$

^aCase 1 is where $A > (B+C)$; 2 is where $A < (B+C)$

Table II. Various cases for four unequal length steps

Case	Conditions ^a
1	$A > (B+C+D)$ and $B > (C+D)$
2	$A > (B+C+D)$ and $(C+D) > B$
3	$(A+D) > (B+C)$, $(B+D) > A$, and $B > (C+D)$
4	$(A+D) > (B+C)$, $(B+C) > A$, $A > (B+D)$, and $B > (C+D)$
5	$(B+C+D) > A$, $A > (B+C)$, and $B > (C+D)$
6	$(A+D) > (B+C)$ and $(C+D) > A$
7	$(A+D) > (B+C)$ and $(B+D) > A > (C+D) > B$
8	$(A+D) > (B+C) > A > (B+D)$ and $(C+D) > B$
9	$(B+C+D) > A > (B+C)$ and $(C+D) > B$
10	$(B+C) > (A+D)$, $(B+D) > A$, and $B > (C+D)$
11	$(B+C) > (A+D)$, $A > (B+D)$, and $B > (C+D)$
12	$(B+C) > (A+D)$ and $(C+D) > A$
13	$(B+C) > (A+D)$ and $(B+D) > A > (C+D) > B$
14	$(B+C) > (A+D)$, $A > (B+D)$, and $(C+D) > B$

^aWhere $A > B > C > D$

Table III. Probability distribution for four unequal length steps.

R-range	Applicability - Case: ^a														$w_4(R)$
	1	2	3	4	5	6	7	8	9	10	11	12	13	14	
0 \rightarrow (A-B-C-D)	x	x													0
0 \rightarrow (-A+B+C-D)										x	x	x	x	x	$\frac{1}{8\pi ABC}$
0 \rightarrow (-A+B+C+D)					x				x						$\frac{-A+B+C+D}{16\pi ABCD}$
0 \rightarrow (A-B-C+D)			x	x		x	x	x							$\frac{(R-A+B+C+D)^2}{64\pi RABCD}$
(A-B-C-D) \rightarrow (A-B-C+D)	x	x													$\frac{8DR - (R+A-B-C+D)^2}{64\pi RABCD}$
(-A+B+C+D) \rightarrow (A-B-C+D)					x				x						
(A-B-C+D) \rightarrow (-A+B+C+D)					x			x							
(-A+B+C-D) \rightarrow (A-B+C-D)										x	x	x	x		
(-A+B+C-D) \rightarrow (-A+B+C+D)											x			x	$\frac{R-A+B+C}{16\pi RABC}$
(A-B-C+D) \rightarrow (A-B+C-D)															
(-A+B+C+D) \rightarrow (A-B+C-D)				x										x	
(A-B+C-D) \rightarrow (-A+B+C+D)			x							x			x		
(A-B+C-D) \rightarrow (A+B-C-D)															$\frac{4CD - (A-B)^2 - (R-C-D)^2}{32\pi RABCD}$

R-range	Applicability - Case: ^a														$W_4(R)$
	1	2	3	4	5	6	7	8	9	10	11	12	13	14	
$(A+B-C-D) \rightarrow (-A+B+C+D)$						x						x			$\frac{-[(R-A-B-C-D)(3R+A+B+C+D) + 4(A^2+B^2+C^2+D^2)]}{64\pi RABCD}$
$(A-B+C-D) \rightarrow (A+B-C-D)$		x						x						x	$\frac{8CD-(R-A+B-C-D)^2}{64\pi RABCD}$
$(A-B+C-D) \rightarrow (A-B+C+D)$	x			x							x				
$(-A+B+C+D) \rightarrow (A+B-C-D)$							x						x		
$(-A+B+C+D) \rightarrow (A-B+C+D)$			x						x						
$(A+B-C-D) \rightarrow (A-B+C+D)$		x						x							$\frac{4CD-(R-A)^2-(B-C-D)^2}{32\pi RABCD}$
$(A-B+C+D) \rightarrow (A+B-C-D)$	x		x	x						x					
$(A+B-C-D) \rightarrow (A+B-C+D)$	x		x	x											$\frac{1}{8\pi RAB}$
$(A+B-C-D) \rightarrow (A+B-C+D)$	x		x	x											
$(A-B+C+D) \rightarrow (A+B-C+D)$		x				x	x	x							$\frac{8CD-(R-A-B+C+D)^2}{64\pi RABCD}$
$(A+B-C+D) \rightarrow (A+B+C-D)$	x	x	x	x	x	x	x	x							
$(A+B+C-D) \rightarrow (A+B+C+D)$	x	x	x	x											$\frac{A+B+C-R}{16\pi RABC}$
$(A+B+C-D) \rightarrow (A+B+C+D)$	x	x	x	x											$\frac{(R-A-B-C-D)^2}{64\pi RABCD}$

^aRefer to Table II for conditions governing each case.

$\text{Cl}^{35}(\text{n},\gamma)\text{Cl}^{36}$ Process

We have utilized this random walk equation to determine the probability distribution and probability of gamma-ray energies resulting from the $\text{Cl}^{35}(\text{n},\gamma)\text{Cl}^{36}$ process. We have chosen, arbitrarily, the 14 gamma-ray cascades listed in Table IV. We then determined $dP_r(R)/dR$ and $P_n(R)$ for each cascade and added them according to the abundances listed in Table IV. These results are depicted in Figs. 1 and 2.

It is of interest to note the "step function" nature of the results of Fig. 1. For example, the jump at 6.24 Mev is a result of the initial contribution from the 7.40 + 1.16 Mev gamma ray cascade. The jump at 6.99 Mev results from the 7.78 + 0.79 Mev cascade.

Table IV. Gamma-ray cascades from $\text{Cl}^{35}(\text{n}, \gamma)\text{Cl}^{36}$

Energies (Mev)	% Occurance
8.55	3.71
7.78, 0.79	10.33
7.40, 1.16	18.54
6.96, 1.60	2.52
6.64, 1.95	15.23
5.72, 2.87	3.84
5.28, 3.34	17.10
6.64, 1.16, 0.79	11.26
6.15, 0.51, 1.95	7.42
5.01, 1.65, 1.95	2.12
6.15, 0.51, 1.16, 0.79	2.38
5.01, 1.13, 0.51, 1.95	1.59
5.01, 1.65, 1.16, 0.79	3.18
5.01, 1.13, 0.51, 1.16, 0.79	0.79

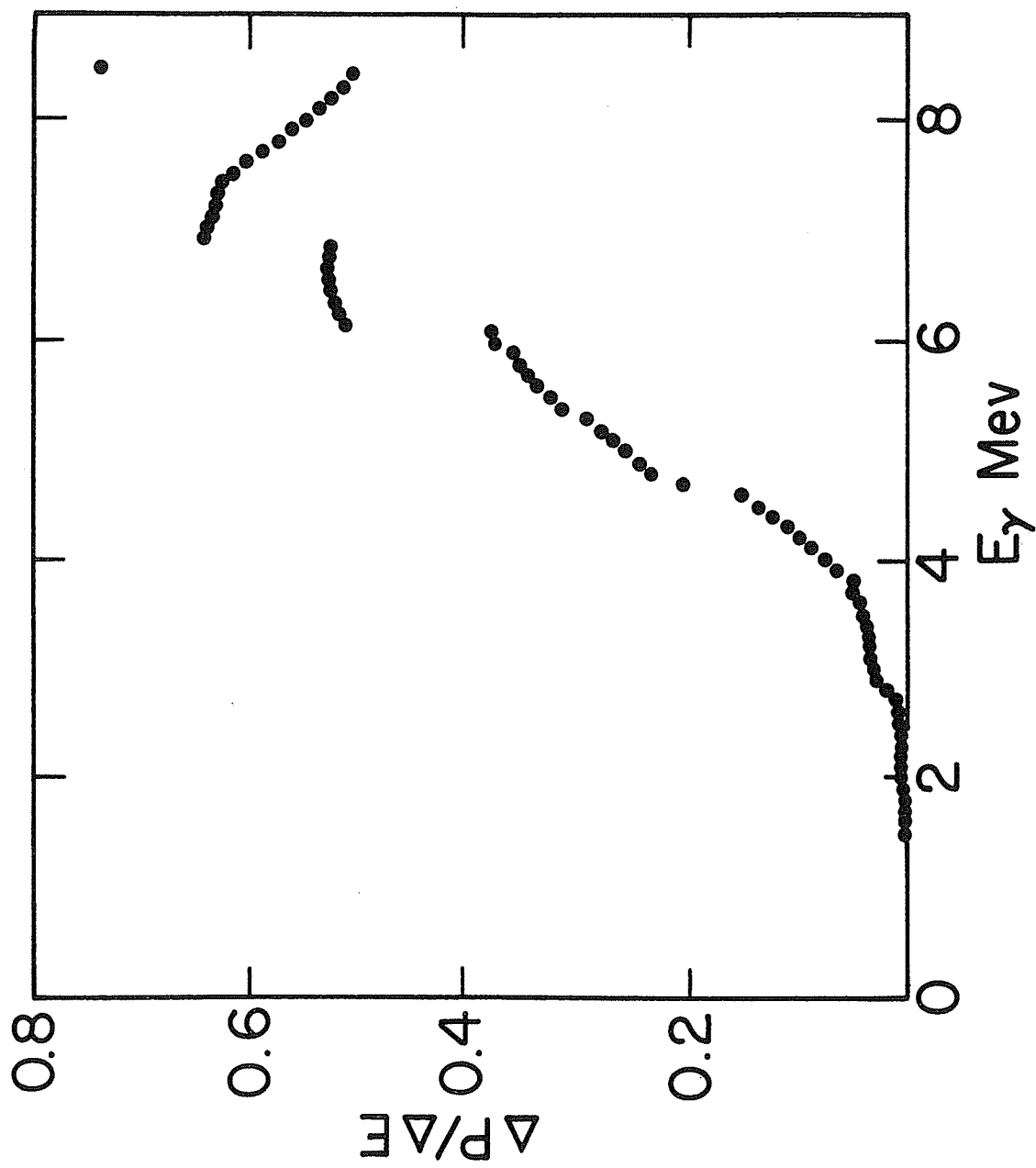


Fig. 1 - Summed Probability Distribution for $\text{Cl}^{35}(n, \gamma)\text{Cl}^{36}$ Gamma-Ray Energies

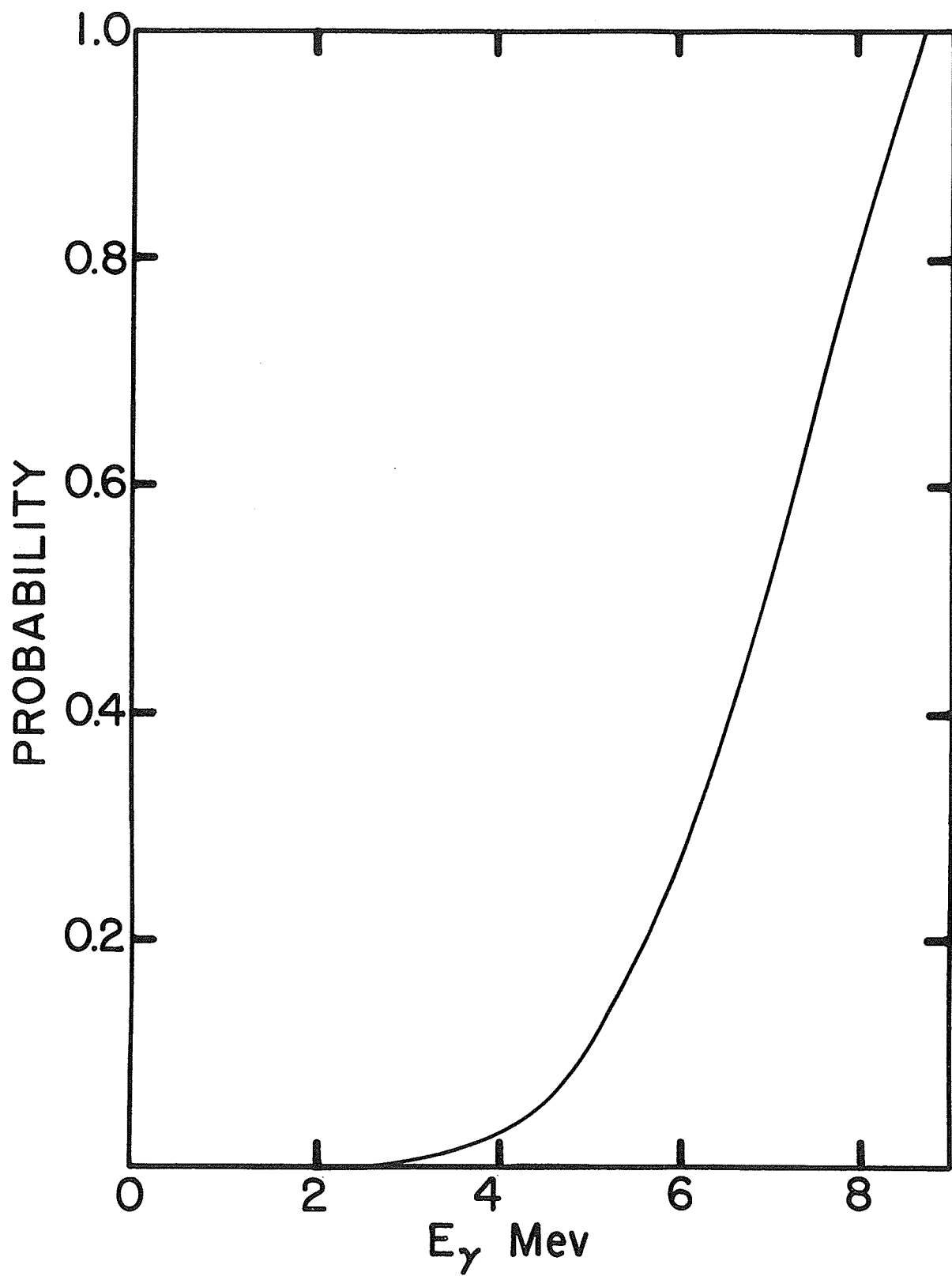


Fig. 2 - Summed Probability for $\text{Cl}^{35}(n,\gamma)\text{Cl}^{36}$ Gamma-Ray Energies

IV. ACTIVATION BY THE (n, γ) PROCESS

If an isolated atom absorbs a thermal neutron and the neutron binding energy is released as a single gamma ray, then, as a result of conservation of momentum, the atom will receive a recoil kinetic energy of²

$$E_r = 537 E_\gamma^2 / m \quad (4)$$

where E_γ is the energy (in Mev) of the gamma quantum, m is the mass (in amu) and E_r is the recoil energy (in ev) of the activated atom. Such energy is usually greatly in excess of thermal energies. For example, the neutron-binding energy associated with the $I^{127}(n,\gamma)I^{128}$ process is 6.6 Mev; an isolated I^{128} atom, releasing this energy as a single gamma ray would acquire 182 ev of kinetic energy.

If the atom which undergoes an (n, γ) reaction is bound chemically, it is not immediately obvious how the gamma-ray recoil is transferred to the atom and the molecule. The observations of Szilard-Chalmers and subsequent experimenters have shown that most of the atoms activated by the (n, γ) process rupture from their parent compound. This indicates that at least a fraction of the gamma-recoil momentum must be deposited in the bond joining the activated atom to the molecule. For a given isotope, the gamma-ray momentum required for bond rupture should depend not only on the bond energy but also on the chemical radical to which the activated atom is bound.

Suess³ calculated that, for a diatomic molecule, the internal energy, E_i , will be increased by

$$\Delta E_i = \left(\frac{537 E_\gamma^2}{m} \right) \left(\frac{M-m}{M} \right) \quad (5)$$

where M is the molecular weight of the molecule.

If a single gamma ray, of the order of 6 Mev energy, is emitted by an atom it would be expected that the activated atom would always rupture from its parent compound. The only exception would be, perhaps, the case where the activated atom was bonded to an atom of small atomic weight as, for example, in the hydrogen halides. However, indirect experimental evidence⁴ indicated that in the (n, γ) activation of gaseous C₂H₅I, of the order of 1% of the I¹²⁸ did not rupture from the parent molecule.

Such failure to bond-rupture can be explained. In (n, γ) activation, and particularly in the activation of the halogens, the neutron binding energy is released most frequently not as a single gamma quantum, but as a gamma-ray cascade. Because of partial cancellation of gamma-ray momenta, some of the atoms could receive a net recoil momentum which is less than that required for bond rupture.

If the complete neutron capture - gamma ray cascade spectrum is known, and if there are no angular correlations between the gamma rays, then, using a closed general solution for three dimensional random walk processes¹, the net gamma-ray momentum probabilities can be calculated. In addition, if the net gamma-ray momentum required for bond rupture can be calculated, then, it is possible to predict the percent of the activated atoms which will fail to rupture from their parent compound.

Unfortunately, at present, the neutron capture - gamma ray data are inadequate to permit calculating the momentum probabilities.

The problem, then, is to determine the manner in which a momentum impulse imparted to an atom is transferred to the bond joining that atom to the molecule.

Steinwedel and Jensen⁵ calculated the fractional distribution of the internal energy between the vibrational and rotational modes of a diatomic molecule. In addition, they considered a quantum-mechanical approach to the problem.

Recently, Svoboda⁶ discussed the relationship between rotational excitation and the bond dissociation energy. Wolfsberg⁷ also included such an effect in his quantum-mechanical evaluation of the beta decay recoil excitation of C¹⁴ labeled ethane.

To calculate the recoil energy required for chemical bond rupture in a polyatomic molecule it is possible to utilize a quantum-mechanical approach similar to that employed by Wolfsberg⁷. However, because of the uncertainties and assumptions associated with such derivations, the calculated value would be considered as only a very rough approximation.

We have considered the problem of recoil momentum activation of polyatomic molecules in terms of kinetic theory. The mathematical model which we propose involves only a small number of well-defined assumptions, and these assumptions, at least for the simpler molecules, may not invalidate the results.

CALCULATION OF MOMENTUM TRANSFER

As indicated in Fig. 3, we visualize the polyatomic molecule as composed of a point-mass atom, A, the remainder of the molecule being a rigid body. The atom, A, is joined to the rigid body by a spring of variable length, r , the spring terminating at C, a point-mass atom of the rigid body. The mass of the components of the rigid body are not considered as concentrated at a point, but retain the spatial configuration present in the molecule. This representation, therefore, does not reduce the problem to that of a diatomic molecule. The important difference is that, unlike a diatomic molecule, the center of gravity of the polyatomic molecule is not necessarily on the line joining the atom, A, to the remainder of the molecule. The center of gravity of the rigid body is at G'; the center of gravity of the molecule is on the line G'A and located at a point G.

The atom, A, receives a momentum impulse, Q . We assume that this impulse causes (a) the molecule to rotate about G, (b) the spring to vibrate, (c) the atom C to rotate about G'.

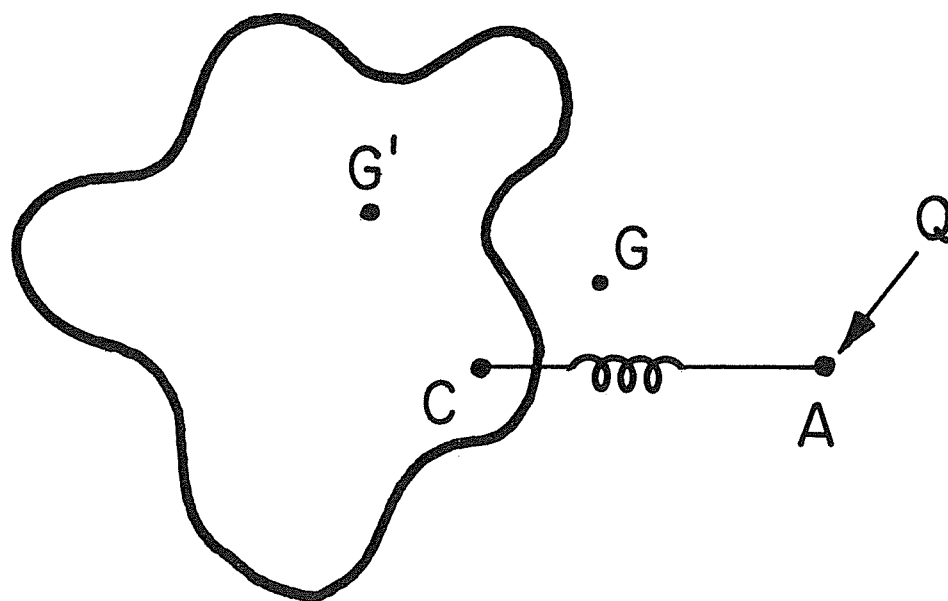


Fig. 3 - Schematic Representation of Pseudo-Polyatomic Molecule

Deposition of Energy

In addition to the terms stated above, we also define:

- M - the molecular weight of the molecule,
- m - the atomic weight of the atom, A,
- m_c - the atomic weight of the atom, C,
- v_A - the velocity of A,
- v' - the velocity of the rigid body attached to A,
- $V(r)$ - the potential energy between the two bodies

The total energy of the system, E_T , is

$$E_T = \frac{1}{2} m v_A^2 + \frac{1}{2} (M-m) (v')^2 + V(r) \quad (6)$$

We further define

$$v = v_A - v' \quad (7a)$$

$$v_G = \frac{m v_A + (M-m) v'}{M} = v' + \frac{m}{M} v \quad (7b)$$

where v_G is the velocity of the center of mass. Eq. 6 may be rewritten

$$E_T = \frac{1}{2} M v_G^2 + \frac{1}{2} \frac{m(M-m)}{M} v^2 + V(r) \quad (8)$$

Since $M v_G^2/2$ is the external energy of the molecule, the internal energy, E_i , is

$$E_i = [m(M-m)v^2/2M] + V(r) \quad (9)$$

Prior to A receiving an impulse, $v_A = v'$ and $r = r_0$. Therefore, $E_i^0 = V(r_0)$. As a result of the impulse, $v_A \neq v'$, the spring undergoes an inelastic stretching, and the separation changes from r_0 to r . The increase in internal energy is

$$\Delta E_i = [m(M-m)v^2/2M] + V(r) - V(r_0) \quad (10)$$

Momentum Transfer

Consider a momentum, Q , randomly directed and acting on the atom, A. This momentum can be resolved into two parts, Q_v - the component along the spring (bond) and Q_r - the component perpendicular to the line joining the atom H to the center of gravity, G' , of the molecule. Vibrational excitation will result from Q_v , rotational excitation from Q_r .

The momentum, Q , may be resolved into the two components as follows.

We choose the location of the atom, A, as the origin; the bond, CA, joining A to the remainder of the molecule as the Z axis, and the center of gravity of the rigid body, G' , as a point on the YZ plane as indicated in Fig. 4. The vector Q is defined by $(|Q|, \theta, \phi)$. Since the component Q_v must lie on the Z axis, Q_r will lie on the plane defined by Q and the Z axis. The vector Q_r is therefore defined by $(|Q_r|, \theta', \phi)$. The vector AG' is defined by $(|AG'|, \alpha, 0)$ and Q_r is perpendicular to AG' . Therefore $\cos \angle (Q_r - AG') = \cos \alpha \cos \theta' + \sin \alpha \sin \theta' \cos \phi$ or $\tan \theta' = -(\cot \alpha / \cos \phi)$

Thus:

$$Q_v = Q \cos \theta + Q(\sin \theta \cos \phi) / \cot \alpha$$

$$Q_r = Q \sin \theta' (\cot^2 \alpha + \cos^2 \phi)^{1/2} / \cot \alpha$$

Assuming that the recoil momentum, Q , is random and isotropic:

$$\langle Q_v^2 \rangle_{Av} = Q^2/3 \cos^2 \alpha \quad (11)$$

$$\langle Q_r^2 \rangle_{Av} = (Q^2/3) + (Q^2/3 \cos^2 \alpha) \quad (12)$$

and $\langle Q_{rx}^2 \rangle_{Av} = \langle Q_{ry}^2 \rangle_{Av} = \frac{1}{2} \langle Q_r^2 \rangle_{Av} \quad (13)$

$$\langle Q_{rz}^2 \rangle_{Av} = 0 \quad (14)$$

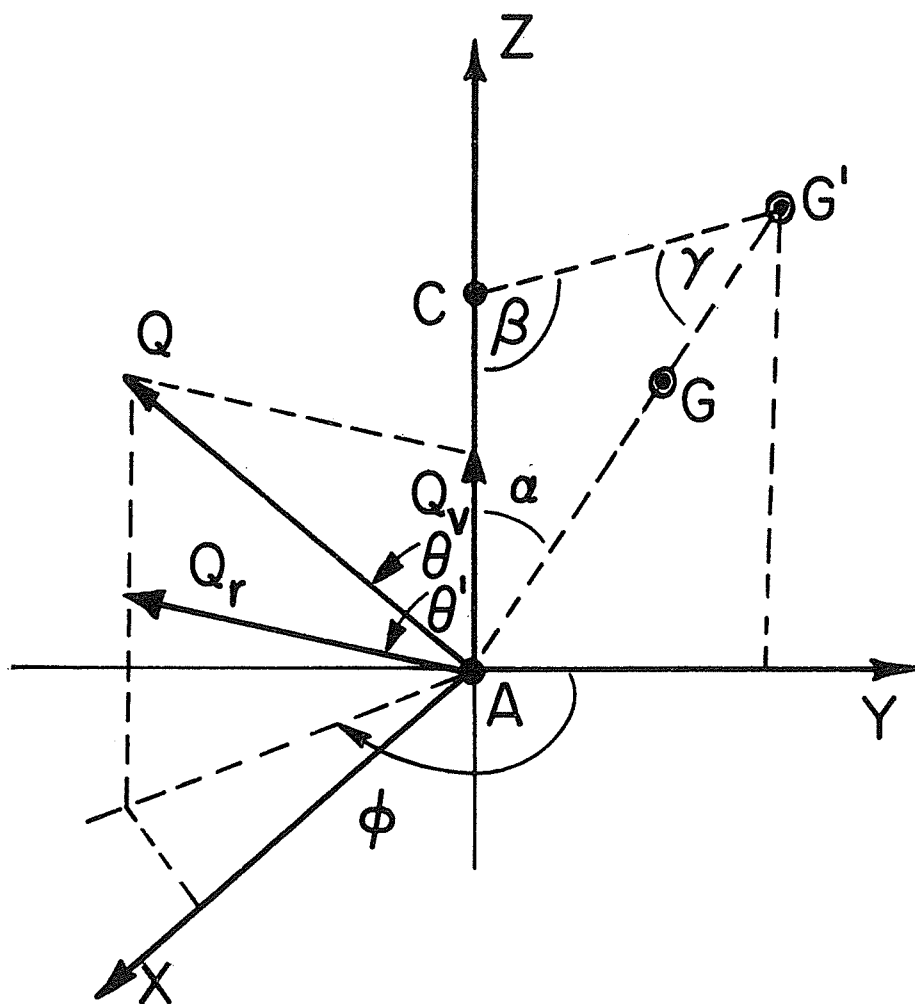


Fig. 4 - General Spatial Coordinates for Pseudo-Polyatomic Molecule

$$\langle Q_{rx} Q_{ry} \rangle_{Av} = 0 \quad (15)$$

Rotational Excitation

According to classical mechanics, the rotational energy of the system is

$$\begin{aligned} \frac{1}{2} \left[I_{xx} \langle W_x^2 \rangle_{Av} + I_{yy} \langle W_y^2 \rangle_{Av} + I_{zz} \langle W_z^2 \rangle_{Av} + I_{xy} \langle W_x W_y \rangle_{Av} \right. \\ \left. + I_{yz} \langle W_y W_z \rangle_{Av} + I_{zx} \langle W_z W_x \rangle_{Av} \right] \text{ where } W_x, W_y, \text{ and } W_z \text{ are the} \\ \text{angular velocities, } I_{xx} = \sum_i m_i (y_i^2 + z_i^2), I_{xy} = -2 \sum_i m_i x_i y_i, \text{ etc.} \\ \text{Since } \langle Q_{rz}^2 \rangle_{Av} = 0, \text{ the rotational energy, } \langle E_r \rangle_{Av}, \text{ is} \end{aligned}$$

$$\langle E_r \rangle_{Av} = \frac{1}{2} \left[I_{xx} \langle W_x^2 \rangle_{Av} + I_{yy} \langle W_y^2 \rangle_{Av} + I_{xy} \langle W_x W_y \rangle_{Av} \right] \quad (16)$$

If the momentum $\langle Q_r \rangle_{Av}$ is consumed totally in rotating the molecule, then

$$\langle W \rangle_{Av} = \frac{\langle Q_r \rangle_{Av}^{(M-m)}}{|AG|mM}, \quad \langle W_x \rangle_{Av} = \frac{\langle Q_{rx} \rangle_{Av}^{(M-m)}}{|AG|mM}, \quad \langle W_y \rangle_{Av} = \frac{\langle Q_{ry} \rangle_{Av}^{(M-m)}}{|AG|mM}$$

$$\langle E_r \rangle_{Av} = \frac{Q^2}{12 m} \left(\frac{M-m}{M} \right)^2 \left[\frac{I_{xx} + I_{yy}}{m|AG|^2} \right] (1 + \sec^2 \alpha) \quad (17)$$

The rotation of the molecule about the center of gravity, G, will result in centrifugal forces acting on the bonds in the molecule. As a first approximation, we assume that the total energy $\langle E_r \rangle_{Av}$ will be associated with the A-C bond. This assumption will be approximately valid in the case where (1) the groups (other than A) attached to C are tightly bound, as in the case

of C-H bonds and (2) the groups (other than C) attached to A are also tightly bound, (3) the center of gravity, G, is on the line, AC. For the "molecule" $\text{CH}_3\text{-NH}_3$, where C is the carbon atom and A is the nitrogen atom, we consider $E_{r\text{ Av}}$ as being deposited totally in the C-N bond. We are in the process of correcting for this approximation. The data presented in Table V (pp. 27-28) are based on this first approximation.

Vibrational Excitation

We may now examine the vibrational excitation. The portion of the molecule attached to A is considered as a rigid body composed of a group of mass points. As this group experiences a recoil momentum, Q_v , it undergoes both rotation and translation. The vector Q_v may be resolved into Q_{vv} which is in the direction of CG' and Q_{vr} which is perpendicular to CG'. Refer to Fig. 5. As a result, $Q_{vv} = Q_v \cos \beta$, $Q_{vr} = Q_v \sin \beta$. The vector Q_{vr} will cause the point mass at C to rotate about G', resulting in a vibration between C and A. Hence

$$E_{vr} = Q_{vr}^2 m_c / 2m(m_c + m) \quad (18)$$

On averaging

$$\langle E_{vr} \rangle_{Av} = Q^2 m_c \sec^2 \alpha \sin^2 \beta / 6m(m_c + m) \quad (19)$$

The vector Q_{vv} will cause the whole group of mass-points to move, thus resulting in a vibration between A and the rigid group of mass points. For this,

$$E_{vv} = Q_{vv}^2 (M-m) / 2Mm \quad (20)$$

On averaging

$$\langle E_{vv} \rangle_{Av} = Q^2 (M-m) \sec^2 \alpha \cos^2 \beta / 6Mm \quad (21)$$

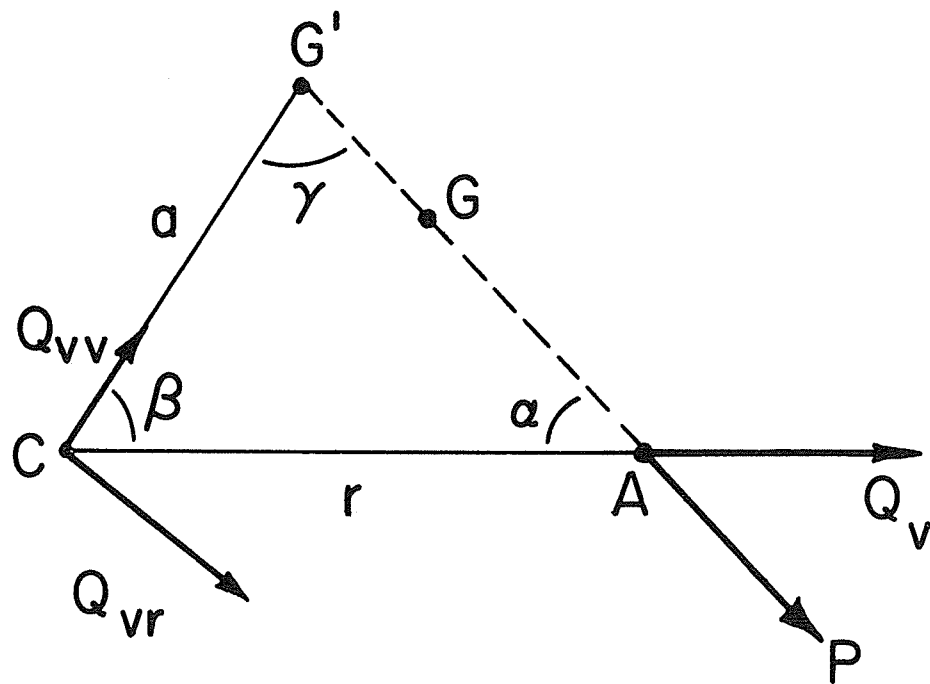


Fig. 5 - Resolution of Q_v Momentum Vector

APPLICATIONS

This derivation is of a general form and thus does not state the manner in which the momentum impulse is imparted to the atom A. The only requirement is that the impulse to A be randomly directed in space. Therefore, we may consider any number of means of activation: (n, γ) recoil, beta-decay, alpha decay, X-ray emission, proton or neutron scattering, etc.

For the specific case of beta decay, Wolfgang, Anderson, and Dodson⁸ have determined the extent of non-rupture in C¹⁴ labeled ethane to be $47 \pm 2\%$. Wolfsberg⁷, using a quantum-mechanical approach calculated that if the recoil energy of the carbon-14 atom is larger than 3.57 ev, the vibrational and rotational energy of the daughter molecule will be larger than the C-N bond energy.

Using the approach outlined above, and considering the CH₃ and NH₃ groups in CH₃-NH₃ as rigid, we calculate that 3.53 ev recoil energy is required.

Similar calculations have been performed for the case of gamma-ray emission from various hydrogen and alkyl halides. Listed in Table V are values for E_r^* , E_{vr}^* , E_{rr}^* , and E_γ required for bond-rupture for compounds where the atom A is Br⁸⁰ or I¹²⁸ and the atom C is (usually) carbon. To calculate these quantities we used Eq. 23 and considered $\langle \Delta E_i \rangle_{Av} = E_b$. On this basis, we defined the fractional contributions as follows:

$$\begin{aligned} E_r^* &= \langle E_r \rangle_{Av} / E_b \\ E_{vr}^* &= \langle E_{vr} \rangle_{Av} / E_b \\ E_{vv}^* &= \langle E_{vv} \rangle_{Av} / E_b \end{aligned}$$

Using Eq. 23, the required gamma-ray energy was calculated after making the substitution:

$$E_\gamma = Q \cdot c \tag{31}$$

where c is the velocity of light.

Table V.
Net Gamma-Ray Energy Required for Bond Rupture

Molecule	E_r^*	E_{vr}^*	E_{rr}^*	E_γ^a Mev
Br ₂	--	--	--	0.771
HBr	--	--	--	6.789
DBr	--	--	--	4.825
TBr	--	--	--	3.968
CH ₃ Br	0.675	0.325	0.000	1.522
CD ₃ Br	0.680	0.320	0.000	1.400
CH ₂ Br ₂	0.823	0.073	0.104	0.880
CF ₃ Br	0.712	0.288	0.000	0.839
CF ₂ Br ₂	0.837	0.113	0.050	0.755
CHClBr ₂	0.849	0.100	0.051	0.742
CCl ₃ Br	0.756	0.244	0.000	0.678
CHBr ₃	0.844	0.123	0.033	0.665
CCl ₂ Br ₂	0.832	0.144	0.024	0.658
CBr ₄	0.802	0.198	0.000	0.542
C ₂ H ₅ Br	0.786	0.058	0.164	1.254
1,1-C ₂ H ₄ Br ₂	0.832	0.097	0.071	0.835
I ₂	--	--	--	0.864
HI	--	--	--	9.762
DI	--	--	--	6.929
TI	--	--	--	5.679
CH ₃ I	0.673	0.327	0.000	2.177

Table V (Cont.)

Molecule	E_r^*	E_{vr}^*	E_{rr}^*	E_γ^a Mev
CD_3I	0.677	0.323	0.000	1.996
CF_3I	0.700	0.300	0.000	1.410
CH_2I_2	0.837	0.093	0.070	1.060
C_2H_5I	0.699	0.184	0.117	1.786
$n-C_3H_7I$	0.804	0.061	0.135	1.485
$i-C_3H_7I$	0.792	0.130	0.078	1.501

^a Calculated according to Eq. 23 for polyatomic molecules and Eq. 25 for diatomic molecules.

EXPERIMENTALLY DETERMINED FAILURE TO BOND-RUPTURE

The purpose of this study was to determine experimentally the extents of failure to bond-rupture of I^{128} and Br^{80} when in the form of alkyl halides. In addition, it was desired to evaluate, if possible, the proposed mathematical model³ describing the transfer of momentum from the gamma rays to the internal modes of the molecules.

Experimental

Quartz bulblets, of 4-5 ml size were filled with about 10-15 mm (if possible) of an alkyl halide and about 700 mm of NO. Generally, 0.1 mm I_2 (or Br_2) was also added. The organic bromides were purified by stirring with concentrated H_2SO_4 followed by washing with water, drying, and distillation. The organic iodides were passed through a silica gel-alumina column and then distilled. The samples were packed in Lusteroid rabbit capsules, thus shielding them from light; if they were not to be irradiated within a few hours, they were stored in a refrigerator.

The samples were irradiated in The University of Michigan megawatt reactor for about 30-45 sec. at a thermal neutron flux of 1.5×10^{12} n/cm²-sec. and an accompanying radiation flux of 5000 r/min.

The nitric oxide served three purposes. (1) It is an efficient radical scavenger and thus, should serve to suppress radiation induced reactions. (2) It should react easily with the Br^{80} atoms dissociating from the alkyl bromides thus preventing the Br^{80} from returning to organic combination. In the case of the I^{128} , it has been shown (Section VII) that NO is an effective moderator for the $I^{128} + CH_4$ reaction, the moderation being due, perhaps, to the fact that NO can effectively neutralize I^+ ions. (3) Large amounts of NO, or, for that matter, any molecular additive, will serve to reduce the kinetic energy of the recoiling halogen atoms before they collide with an organic halide molecule

and thus assist in preventing these atoms from re-forming organic compounds.

Since it was expected that the extent of failure to bond-rupture would be 1% or less, it was of utmost importance to be able to separate completely the dissociated halogen from the organic halide. To accomplish this, the following procedure was used.

After irradiation, the bulbs were broken in a separatory funnel beneath an aqueous solution of Na_2SO_3 ; chloroform containing a small amount of I_2 was added immediately and the mixture shaken to extract organic halides. The two phases were each counted for a period of about 20 minutes, and, after correcting for coincidence-loss and density effects, the percent of the total activity found in the organic phase was calculated.

The extraction procedure was evaluated by irradiating mixtures of $\text{NO} + \text{I}_2$ and $\text{NO} + \text{Br}_2$ and determining the percent activity found in the organic phase. The results were approximately 0.01% for I^{128} and 0.004% for Br^{80} . Thus, any observed organic activity greater than these values is not due to inorganic halogen dissolved in the organic phase.

Results and Discussion

Listed in Table VI are the observed values of the percent of the halogen activity found in the organic phase. The uncertainty is calculated in terms of the standard deviation of the mean.

Let us assume that the I^{128} or Br^{80} splits from a molecule only if it receives a net gamma-recoil momentum sufficient to cause carbon-halogen bond rupture. If this be so, then, for a series of molecules, a plot of the percent failure to bond rupture vs. the calculated net gamma-ray energy required for bond rupture (Table V) should be identical with a plot of the gamma-ray energy probability vs. the net gamma-ray energy.

Table VI.
Experimentally Determined Failure to Bond-Rupture

Molecule	Percent Halogen found as Organic	Average ^a
CH ₃ Br	0.23, 0.29, 0.27, 0.22, 0.25, 0.23, 0.262, 0.25, 0.232	0.25 ± 0.01
CD ₃ Br	0.28, 0.26, 0.22, 0.16, 0.16, 0.16, 0.17, 0.18	0.20 ± 0.02
CH ₂ Br ₂	0.150, 0.208, 0.195, 0.160, 0.060, 0.130, 0.072, 0.079, 0.162, 0.160, 0.100, 0.172, 0.150, 0.202, 0.020, 0.014, 0.120, 0.093, 0.080, 0.097, 0.130, 0.091, 0.093, 0.103, 0.092, 0.046.	0.115 ± 0.010
CF ₃ Br	0.090, 0.110, 0.100, 0.098, 0.099, 0.093, 0.120, 0.115, 0.123	0.105 ± 0.004
CF ₂ Br ₂	0.105, 0.112, 0.086, 0.088, 0.082, 0.091, 0.089	0.093 ± 0.004
CHClBr ₂	0.090, 0.092, 0.109, 0.083, 0.091, 0.068, 0.075	0.087 ± 0.005
CCl ₃ Br	0.057, 0.072, 0.051, 0.062, 0.079, 0.080, 0.061	0.066 ± 0.004
CHBr ₃	0.089, 0.030, 0.044, 0.028	0.048 ± 0.013

Table VI (Cont.)

Molecule	Percent Halogen found as Organic	Average ^a
CBr ₄	0.032, 0.051, 0.034, 0.044 0.026	0.031 ± 0.006
C ₂ H ₅ Br	0.31, 0.28, 0.41, 0.38, 0.31, 0.26, 0.45, 0.21	0.33 ± 0.03
1,1-C ₂ H ₄ Br ₂	0.157, 0.175, 0.151, 0.183, 0.200	0.173 ± 0.009
CH ₃ I	1.10, 1.10, 0.99, 1.00, 1.14, 1.05, 1.24	1.09 ± 0.03
CD ₃ I	1.03, 1.02, 1.12, 0.45, 0.56, 0.94, 0.65, 0.56, 0.52, 0.43, 0.23, 0.45, 0.71, 0.99, 0.56, 0.65	0.68 ± 0.06
CF ₃ I	0.176, 0.158, 0.118, 0.112, 0.083, 0.091	0.12 ± 0.02
CH ₂ I ₂	0.06, 0.07, 0.08, 0.056, 0.07, 0.070	0.068 ± 0.004
C ₂ H ₅ I	0.87, 0.90, 0.82, 0.76, 0.71, 0.82, 0.75, 1.01, 1.05, 0.57, 0.96, 0.64	0.82 ± 0.04
n-C ₃ H ₇ I	0.81, 0.84, 0.72, 0.62, 0.86, 0.85, 0.54, 0.58, 0.48, 0.44, 0.55	0.66 ± 0.05
i-C ₃ H ₇ I	0.14, 0.46, 0.26, 0.32, 0.34	0.30 ± 0.05

^a Uncertainty is the standard deviation of the mean.

Since, for these isotopes, the neutron capture - gamma data are inadequate to permit calculating the probabilities, the latter plot cannot be obtained. However, the general shape of the probability curve will, perhaps, be similar to that calculated for the $\text{Cl}^{35}(\text{n},\gamma)\text{Cl}^{36}$ process. This calculated curve is depicted in Fig. 2. Plotted in Figs. 6 and 7 are the observed failure to bond-rupture vs. the calculated minimum recoil gamma-ray energy.

It will be noted that the data for the methyl iodides and bromides do appear to lie on a smooth curve.

From Figs. 6 and 7 we may deduce that the expected failure to bond-rupture of I_2 is 0.04% and that of Br_2 is 0.08%.

The data for $\text{C}_2\text{H}_5\text{Br}$, 1,1- $\text{C}_2\text{H}_4\text{Br}_2$, $\text{C}_2\text{H}_5\text{I}$, n- $\text{C}_3\text{H}_7\text{I}$, and i- $\text{C}_3\text{H}_7\text{I}$ deviate markedly from the curve drawn through the methyl-halide data. Apparently, as stated above, the direct use of $E_{\gamma, \text{Av}}$ is to be considered as only a first approximation. It would be expected to be most in error for the higher carbon-content compounds. Preliminary calculations correcting for the assumption indicate that these ethyl and propyl compound data will be more in accord with the methyl data.

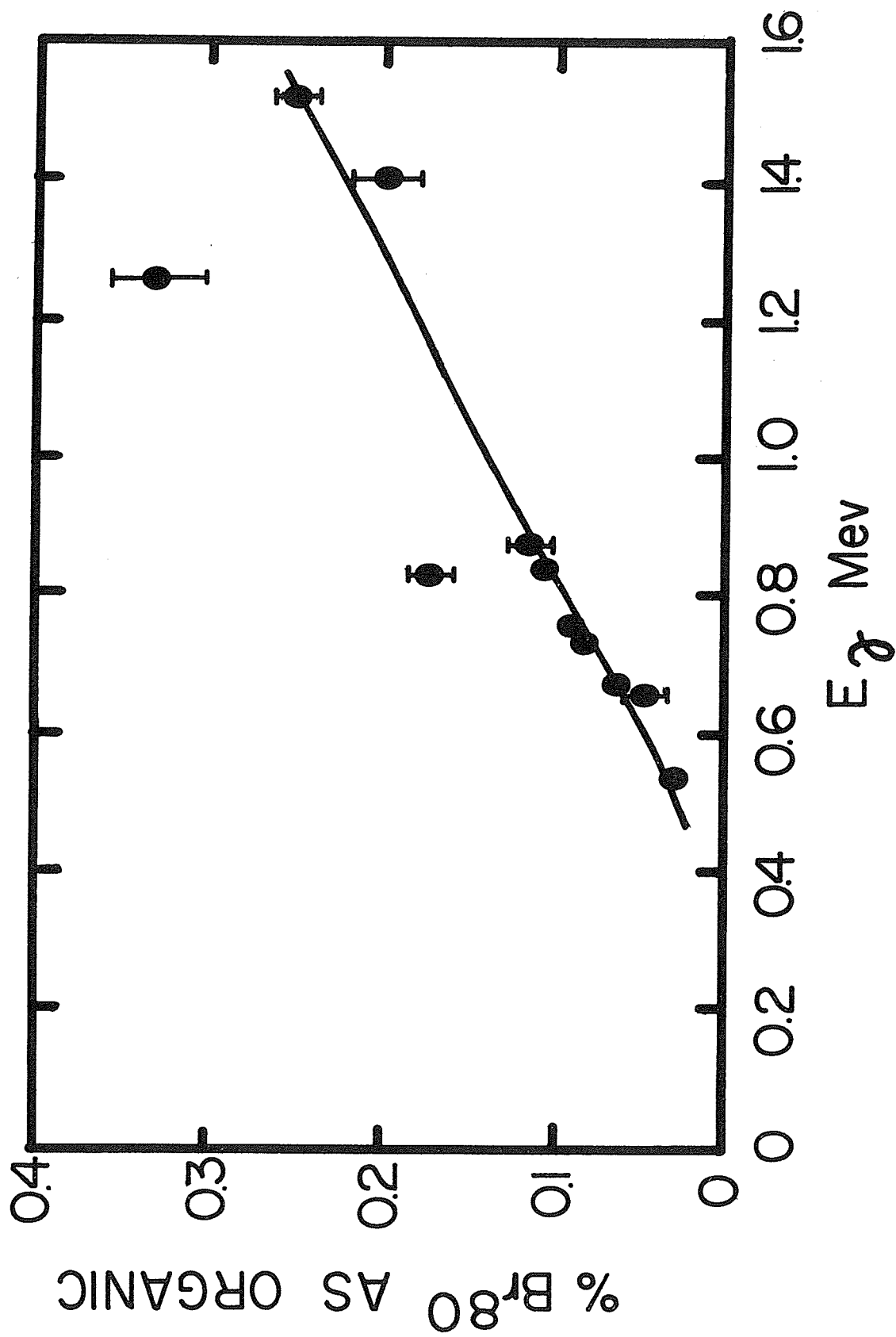


Fig. 6 - Br^{80} Failure to Bond-Rupture as a Function of Required Net Gamma Recoil Energy

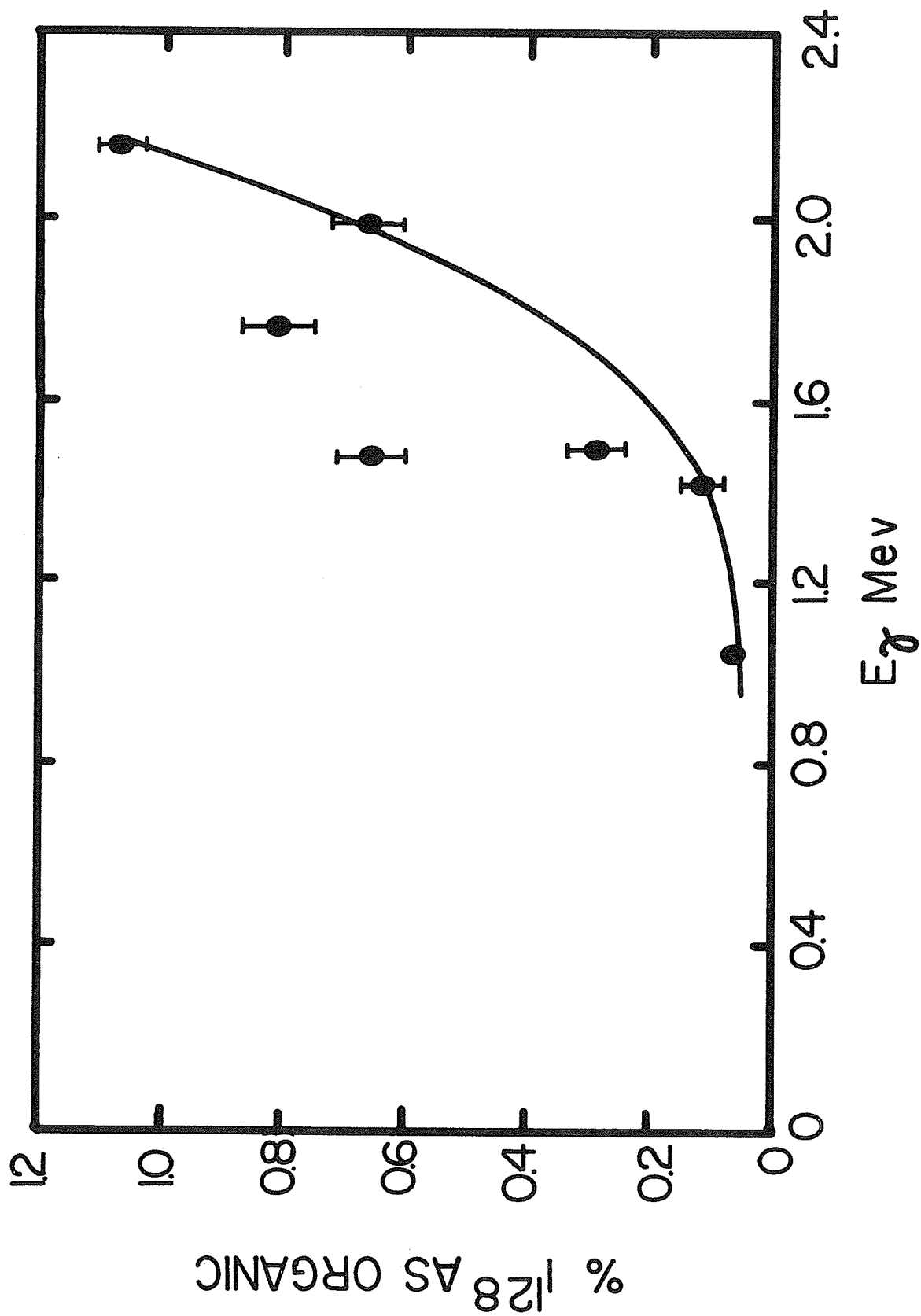


Fig. 7 - I^{128} Failure to Bond-Rupture as a Function of Required Net Gamma Recoil Energy

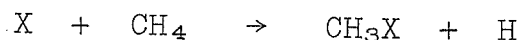
V. KINETIC THEORY OF HOT-ATOM REACTIONS

Estrup and Wolfgang⁹ (E-W) have developed a kinetic theory of hot-atom reactions based partially on the mathematics of neutron cooling processes. One of the assumptions made by E-W is that the activated atoms are formed with an initial kinetic energy which is greatly in excess of that required for reaction. Therefore, on the average, the hot atoms undergo a number of collisions and assume a statistically-defined distribution of energies prior to reaction. To utilize this theory in our studies it is necessary that the Br^{80} and I^{128} atoms or ions also form a statistical distribution of energies.

Referring to the data of Figs. 6 and 7 we know that there results partial cancellation of gamma-recoil momenta in cascade gamma emission. The Br^{80} atoms will be formed with a distribution of energies ranging from some low value to a maximum of about 357 ev. For I^{128} the maximum is about 182 ev. We therefore assume that there results an approximate statistical distribution of energies.

In addition, two additional assumptions stated by E-W must apply. They are: (1) that energy loss occurs as a result of elastic-sphere collisions; that the minimum energy required for reaction is large compared with thermal energies.

For reactions of the type:



where X is a Br^{80} or I^{128} atom or ion the energy required for reactions vary from about 1.2 to about 15 ev.

To utilize the E-W theory it is necessary to have available data concerning the extent of production of a given compound as a function of the mole-fraction of the target atom. For the reactions of Br^{80} or I^{128} with gaseous methane, the principal organic products are, respectively, $\text{CH}_3\text{Br}^{80}$ and $\text{CH}_3\text{I}^{128}$. Thus, the percent organic activity as a function of the mole-fraction CH_4 can be taken as an indication of the percent $\text{CH}_3\text{Br}^{80}$ or $\text{CH}_3\text{I}^{128}$.

The E-W theory involves two variables, α and f . The quantity α is the average logarithmic energy loss per collision and is a function of the mass of the hot atoms and the mass of the molecule or atom with which the hot atom collides. The quantity f is the probability that the collision be with CH_4 and is a function of the mole-fractions of the components and the cross-sections for the various collisions.

For a system composed of a single reactant:

$$\begin{aligned} & (\alpha/f) \cdot (\text{fraction of the activity in a given form}) \\ & = I - (f/\alpha)K \end{aligned} \tag{32}$$

According to the above equation, a plot of $(\alpha/f)(\text{fraction Br}^{80} \text{ or I}^{128} \text{ as organic})$ versus f/α should approximate a straight line and, equally important, all points should fall on the same line regardless of the moderator used.

VI. Br^{80} ACTIVATED BY THE (n,γ) REACTION

We have investigated the reaction of Br^{80} with gaseous methane in an attempt to determine whether the reaction occurs principally because of the positive charge or because of the gamma-recoil kinetic energy acquired by the Br^{80} .

If the positive charge is responsible for the reactivity of the Br^{80} , then different extents of reaction with CH_4 would be expected for (n,γ) activated $\text{Br}^{80\text{m}}$ and Br^{82} since 12 and 25%, respectively, of these isotopes are positively charged¹⁰. A single experiment⁹ indicated that both Br^{80} and $\text{Br}^{80\text{m}}$ react with CH_4 to produce the same percent of organic activity. In gaseous mixtures of Br_2 and $\text{C}_6\text{H}_5\text{Br}$, C_6H_6 , or $n\text{-C}_3\text{H}_7\text{Br}$ the percent organic activity was also found to be the same for the three isotopes¹⁰. The lack of an isotope effect in these latter experiments could be due, however, to the fact that the ionization potential of the main component of each system is less than that of Br .

Experimental

Quartz bulblets, 4-5 ml. in size, were filled with additive, CH_4 , and 2 mm. Br_2 , so that the total pressure was (generally) about 1 atm.

The samples were irradiated in the University of Michigan megawatt reactor for approximately 2 sec. at a thermal neutron flux of 1.5×10^{12} n/cm²-sec. and an accompanying gamma radiation flux of 8000 r/min. Because of the presence of scavenger Br_2 , there occurred negligible radiation induced effects.

The samples were broken in a separatory funnel beneath a two phase mixture of CHCl_3 and I_2 , and aqueous Na_2SO_3 . The two portions were counted to determine the activity in each phase and after correcting for $\text{Br}^{80\text{m}}$ content and counting coincidence and density effects, the percent of the total activity present in the organic phase was determined.

Results

The percent of the Br^{80} present as organic activity for the various systems are listed in Table VII.

To interpret correctly the data where the bromine was present as $\text{C}_2\text{H}_5\text{Br}$, it is necessary to realize that a small fraction of the Br^{80} will not split from the $\text{C}_2\text{H}_5\text{Br}^{80}$ molecule and thus will be recorded as organic activity. This failure to bond rupture, which amounts to 0.33%, must be subtracted from these data of Table VII. In addition, the Br^{80} could react with the molecular additives and contribute to the observed organic activity. Thus, it is necessary to correct further these data of Table VII for the fractional reactivity with the molecular additives. To do this, we subtracted from the observed values the product of the mole fraction of the additive, multiplied by the extent of reaction with essentially pure additive to produce organically bound Br^{80} . These maximum extents of reaction to produce organic Br^{80} are, correcting for any failure to bond rupture: CF_4 - 0.7, C_2F_6 - 3.0, and $\text{C}_2\text{H}_5\text{Br}$ - 2.2%.

These corrected data of Table VII are depicted graphically in Figs. 8 and 9. The solid curves are calculated according to the Estrup-Wolfgang theory⁹. In order to avoid confusion, the uncertainties have been omitted from these figures.

Extrapolating the data for the systems where the mole fraction of the additive was less than 0.1, it was found that at zero mole-fraction additive $13.3 \pm 0.5\%$ of the Br^{80} reacts with CH_4 to become stabilized in organic combination. The only other determination of this quantity was made by Gordus and Willard⁴ and indicated 18% Br^{80} as organic. The reason for this difference is probably due to the presence of radiation-induced reactions in their experiments. The gamma dose received by their samples was almost 100 times that received by our samples.

Table VII

Percent Br⁸⁰ Stabilized in Organic
Combination in Various Gaseous Mixtures^a

Additive	Pressure CH ₄ (mm)	Pressure Additive (mm)	Mole Fraction Additive ^{b,c}	Percent Br ⁸⁰ as Organic ^d
He	654	27	0.040(7)	13.5(2)
				13.6(4)
	549	83	0.131(2)	12.6(1)
				12.6(2)
	440	87	0.165(5)	12.0(2)
				12.0(2)
	127	300	0.703(123)	8.5(4)
				9.2(4)
Ne	416	52	0.111(12)	11.2(4)
				12.5(3)
	454	129	0.221(17)	10.8(3)
	239	217	0.476(52)	9.6(2)
	239	219	0.478(52)	8.6(4)
Ar	501	127	0.202(26)	12.1(5)
				12.2(5)
	238	177	0.427(35)	5.5(6)
				6.7(4)
	148	279	0.653(40)	4.8(6)

Table VII (Con't.)

Additive	Pressure CH ₄ (mm)	Pressure Additive (mm)	Mole Fraction Additive ^{b,c}	Percent Br ⁸⁰ as Organic ^d
Kr	649	41	0.059(1)	11.5(3)
				11.5(4)
	589	97	0.141(2)	8.7(4)
				8.9(3)
	283	147	0.342(3)	5.3(2)
				5.6(2)
	106	91	0.462(7)	3.6(3)
				3.6(1)
Xe ^e	663	20	0.029(2)	11.8(3)
				14.2(2)
	662	43	0.061(1)	11.3(4)
				13.8(4)
	568	60	0.096(1)	9.8(3)
				10.0(4)
	335	62	0.156(2)	6.9(3)
				8.0(4)
CF ₄	557	90	0.139(2)	5.1(5)
				4.7(5)
	437	241	0.356(3)	8.0(2)
				8.4(3)
	262	438	0.626(5)	4.7(2)
				5.0(3)
				2.8(1)
				3.4(1)

Table VII (Con't.)

Additive	Pressure CH ₄ (mm)	Pressure Additive (mm)	Mole Fraction Additive ^{b, c}	Percent Br ⁸⁰ as Organic ^d
C ₂ F ₆	498	143	0.223(2)	6.3(3)
	368	275	0.428(3)	5.2(2)
				6.6(2)
Br ₂	714	2	0.003(1)	13.1(7)
				14.3(6)
	658	3	0.005(1)	13.4(4)
	656	23	0.034(7)	11.3(3)
				13.0(2)
	629	65	0.096(7)	10.4(1)
				10.9(2)
	268	65	0.195(15)	6.6(1)
				7.2(1)
C ₂ H ₅ Br ^f	112	63	0.360(29)	3.2(1)
				4.4(1)
	699	11	0.015(4)	12.8(4)
				13.1(4)
	657	20	0.029(1)	12.4(4)
				13.4(3)
	467	22	0.045(2)	11.1(3)
				11.6(3)
	323	23	0.067(3)	10.5(2)
				12.1(3)
	213	26	0.109(4)	9.0(7)
				9.1(2)

Table VII (Con't.)

Additive	Pressure CH ₄ (mm)	Pressure Additive (mm)	Mole Fraction Additive ^{b,c}	Percent Br ⁸⁰ as Organic ^d
C ₂ H ₅ Br ^f	360	93	0.205(2)	7.2(1)
				7.5(1)
	183	101	0.356(5)	5.8(1)
	179	149	0.454(5)	5.4(1)
				5.5(1)

(a) All samples, except where noted, contained 2 mm. Br₂.

(b) Calculated assuming additive pressures.

(c) Uncertainty in last figure or figures (given in parenthesis) is based on estimates of determining individual pressures.

(d) Uncertainties (given in parenthesis) based on estimates of uncertainty in positioning 18.6 min. slope through decay data for inorganic and organic fractions for each run.

(e) Samples contained 2 mm. C₂H₅Br and 0.2 mm. Br₂.

(f) 0.2 mm. Br₂ scavenger present.

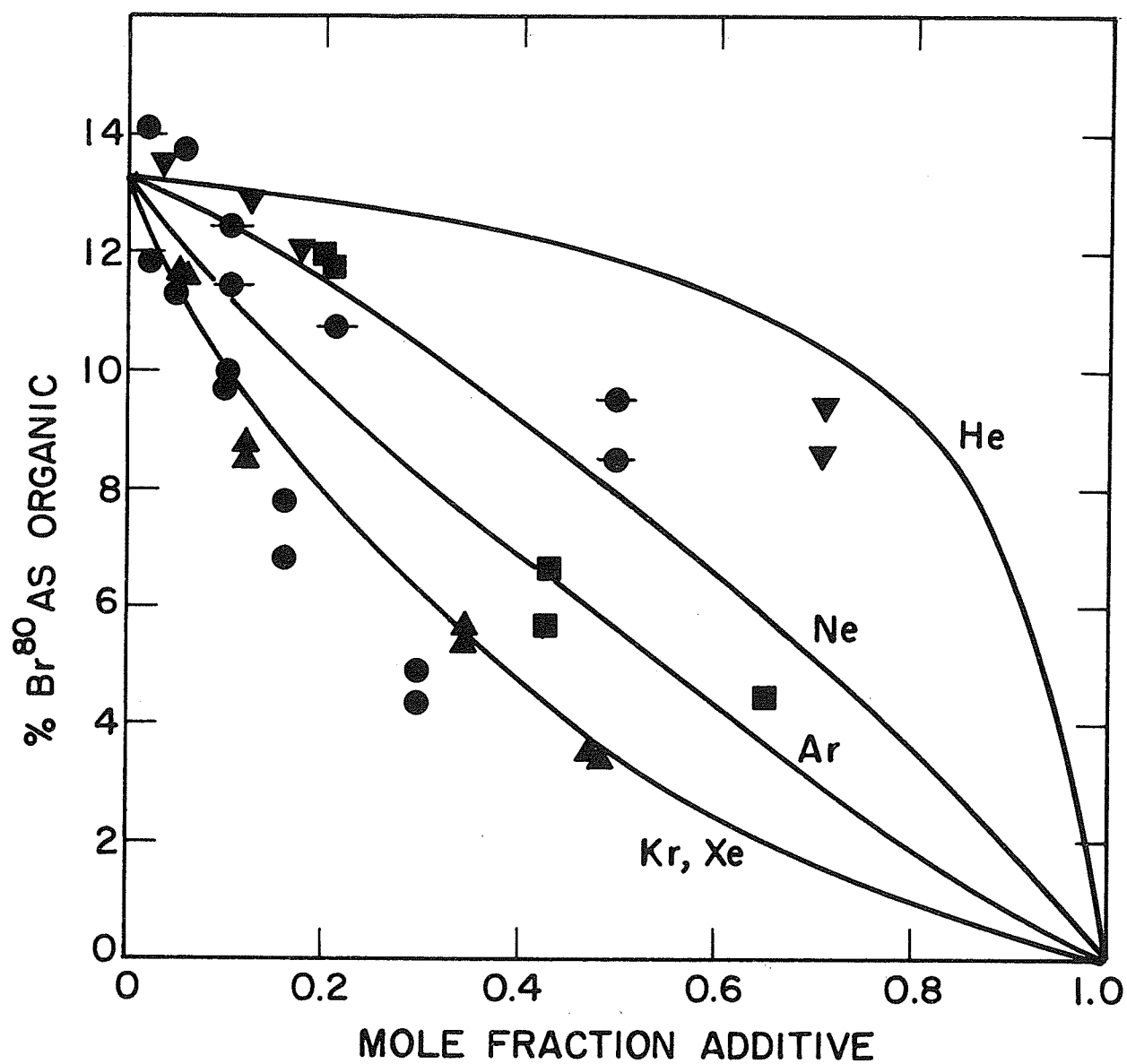


Fig. 8 - Effect of inert-gas moderators on the reaction of gaseous CH_4 with Br^{80} activated by the (n, γ) process. Moderators: helium, ∇ ; neon, \bullet ; argon, \blacksquare ; krypton, \blacktriangle ; xenon, \bullet .

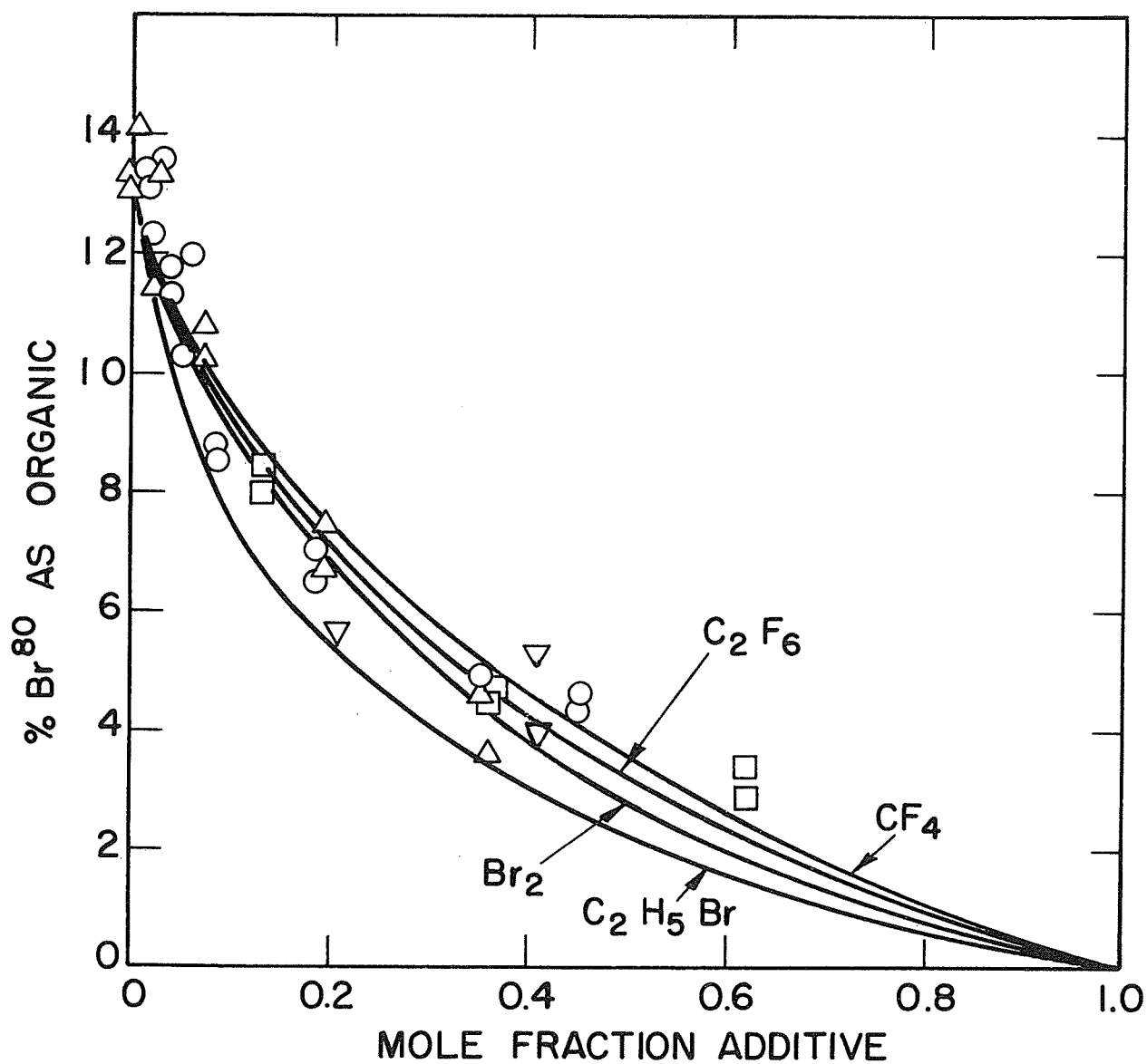


Fig. 9 - Effect of molecular moderators on the reaction of gaseous CH_4 with Br^{80} activated by the (n,γ) process. Moderators: CF_4 , \square ; C_2F_6 , ∇ ; Br_2 , \triangle ; $\text{C}_2\text{H}_5\text{Br}$, \circ .

Discussion

It should be possible to interpret qualitatively the effects of the different moderators. There are various ways in which the $\text{Br}^{80} + \text{CH}_4$ reaction can be moderated, depending upon the nature of the Br^{80} and the moderator: (1) removal of the Br^{80} kinetic-energy; (2) neutralization of Br^{80} ions; (3) inelastic collisions resulting in the quenching of excited Br^{80} ions or atoms; (4) reaction of Br^{80} with the additive, the Br^{80} becoming stabilized in chemical combination.

Inert gases cannot moderate via process 4. In addition, inert gases are found to be inefficient in quenching excited species¹¹ and because of their high ionization potentials are very inefficient in undergoing charge-transfer with Br^+ ions. Therefore, if moderation of the reaction by the inert gases occurs, it must be due mainly to process 1.

We may next examine the experimental data for the samples containing inert gases. Referring to Fig. 8 and ignoring the solid curves, it is seen that each inert gas is capable of suppressing the extent of formation of organic Br^{80} . If the inert gases moderate the reaction principally via process 1, then the relative effectiveness of the additives would depend on the size of the inert gas atoms and on the fractional energy transfer per Br^{80} -inert gas collision. Thus, a plot such as Fig. 8 should indicate that the moderating efficiencies increase in the order: He, Ne, Ar, Kr-Xe. As seen, the data of Fig. 8 are in accord with that expected for kinetic-energy moderation.

We may also attempt to determine qualitatively whether the formation of organic Br^{80} is due totally to hot processes. This may be accomplished by extrapolating the data of Fig. 8 to zero mole fraction CH_4 . If, for example, the data extrapolated to 6%, such data would suggest that 6% of the organic Br^{80} is formed via thermal processes and $13.3 - 6 = 7.3\%$ via hot processes. The data for Ar, Kr, and Xe, however, extrapolate to about 0 ± 2 percent and there is no reason to expect the helium and neon data to extrapolate to a value which differs from that of the other inert-

gases. Therefore, it would appear that the organic Br^{80} is formed principally via hot reactions.

The molecular additives are capable of moderating according to all four processes. However, as with the inert-gases, we may eliminate certain processes from consideration.

Molecular Br_2 and $\text{C}_2\text{H}_5\text{Br}$ should be able to moderate efficiently via all four processes.

For CF_4 we would expect charge-transfer to be a very inefficient process¹² since the ionization potential of CF_4 (probably about 13 ev) is greater than that of Br. This compound has been found to be highly inefficient in quenching excited I^{128} ions (Section VII). Therefore, it might also be expected that CF_4 should be inefficient in quenching excited Br^{80} atoms or ions. Reactions of Br^{80} atoms or ions with CF_4 to yield inorganic or organic Br^{80} are more endothermic than similar reactions of Br^{80} with CH_4 . Therefore, it is possible that the Br^{80} would react preferentially with CH_4 . This conclusion is substantiated by the fact that the reaction of Br^{80} with excess CF_4 results in only 0.7% Br^{80} as organic, whereas 13.3% Br^{80} as organic is found in the $\text{Br}^{80} + \text{CH}_4$ reaction. In addition, the endothermicities for the reaction with CF_4 to form inorganic and organic Br^{80} are of the same order magnitude (80-90 kcal). As an approximation, it is possible that only about 0.7% Br^{80} as inorganic would result in the reaction with CF_4 . Since processes 2, 3, and 4 are probably of minor importance, we would expect CF_4 to moderate principally via process 1.

Similar arguments may be presented for C_2F_6 moderation. On the basis of experiments with I^{128} , quenching should be unimportant. Because of the high endothermicities and the low extent of production of organic Br^{80} (3%), reaction of Br^{80} with C_2F_6 to yield inorganic Br^{80} may also be of minor importance. The ionization potential of C_2F_6 is not available in the literature; however, it is probably of the order of 11.7-12 ev. Since the ionization potential of Br is 11.84 ev, charge-exchange could be possible. Removal of kinetic-energy, process 1, could also occur.

Experimentally, it is observed that the moderation exhibited by all the molecular additives is quite similar to that exhibited

by krypton and xenon. It was seen from the inert-gas data that thermal processes are of little importance. The ionization potentials, quenching abilities, etc., and the chemical reactivities toward bromine atoms or ions vary greatly among the molecular additives. Since similar moderation efficiencies result from substances of similar molecular or atomic weights (xenon, krypton, and the molecular additives), these data would suggest that, for the molecular additives, processes 2, 3, and 4 are not as important as kinetic-energy transfer. Thus, it would appear that the reaction of Br^{80} with CH_4 proceeds mainly via a mechanism involving hot Br^{80} atoms.

Figure 10 is a plot of the experimental data corresponding to Eq. (32) given in Section V. In addition, for essentially pure methane, $f/\alpha = 2.84$ and $(\alpha/f) \cdot (\text{fraction of } \text{Br}^{80} \text{ as organic}) = 0.0470$. The best straight line drawn through the data and ending at the point (2.84, 0.0470) has an intercept $I = 0.057 \pm 0.005$ and a slope $-K = -(0.0035 \pm 0.0020)$. It should be emphasized that the points for all moderators, with the possible exception of $\text{C}_2\text{H}_5\text{Br}$, appear to approximate the same line. The upward trend exhibited by the $\text{C}_2\text{H}_5\text{Br}$ data could be due, in part, to an incorrect choice of the value of the apparent diameter of the compound.

The solid curves of Figs. 8 and 9 were calculated using Eq. (32) and the above values of K and I . It is seen that the curves for Xe and Kr moderation are identical. This is due to the fact that, whereas the Xe-Br cross-section is larger than that of the Kr-Br, per collision, because of the similarity in atomic weights, krypton is capable of removing, on the average, more energy from Br^{80} than is xenon. It should also be noted that this kinetic theory results in curves for the molecular additives (Fig. 9) which are in reasonable agreement with the data. This suggests, as do the data of Fig. 10, that the molecular additives serve mainly to remove Br^{80} excess kinetic energy. If moderation by the molecular additives were via a process other than kinetic-energy removal, it would only be under the most fortuitous circumstances that their moderation data would be described by the kinetic-theory curves.

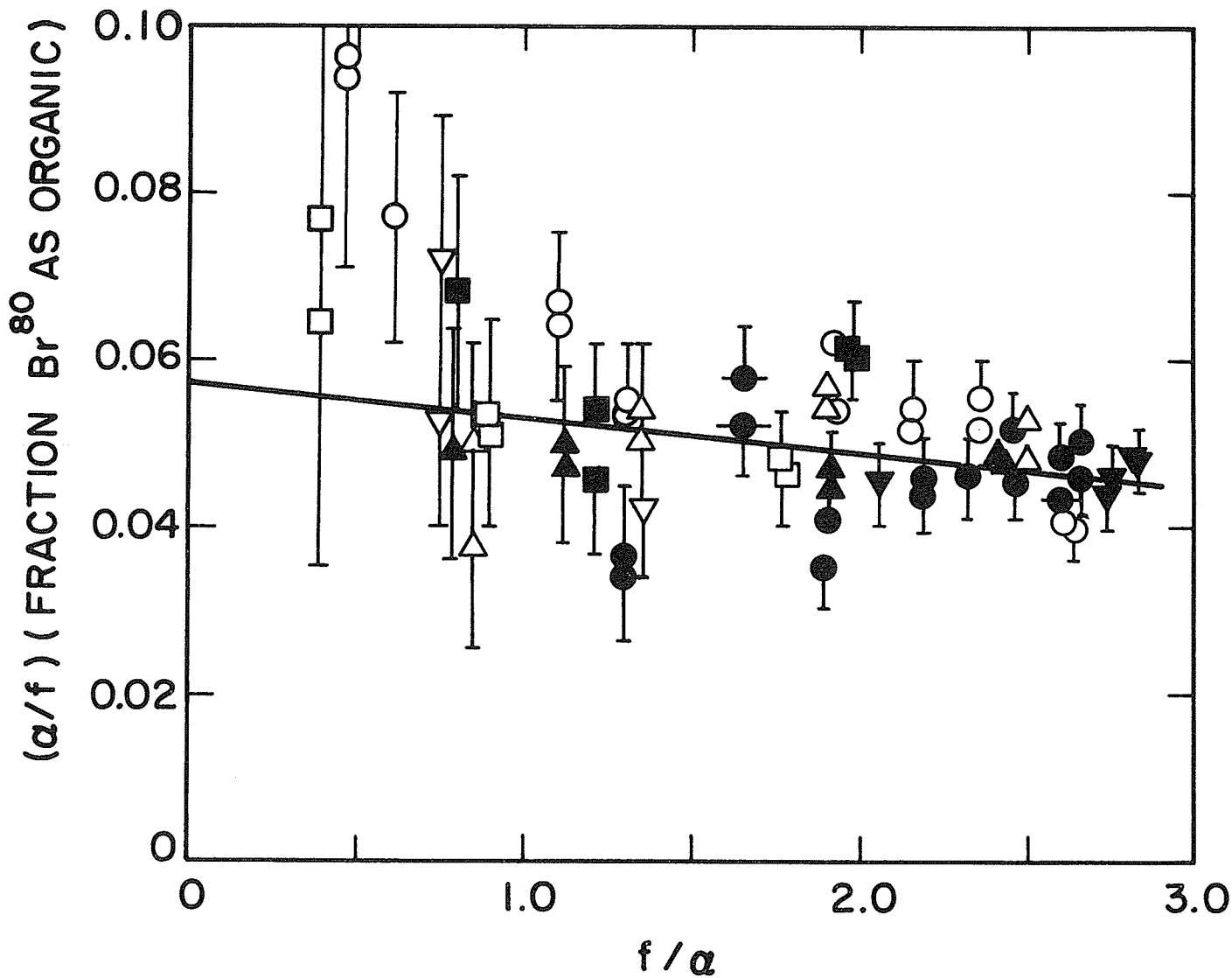


Fig. 10 - Plot corresponding to equation 32 for the Br^{so} in organic combination. Moderator symbols are listed in captions for Figs. 8 and 9.

In summary, the data of Fig. 10 would tend to support the conclusion stated earlier that the reaction of Br^{80} with methane occurs principally, if not completely, as a result of the gamma-recoil kinetic energy acquired by Br^{80} .

VII. I^{128} ACTIVATED BY THE (n,γ) REACTION

Hornig, Levey, and Willard¹³ determined that I^{128} produced by the $I^{127}(n,\gamma)I^{128}$ process is able to react with gaseous methane to form CH_3I^{128} . Further investigations by Levey and Willard¹⁴ indicated that molecules with ionization potentials lower than that of an iodine atom are more effective than inert gases in moderating the $I^{128} + CH_4$ reaction. They interpreted these data as indicating that the positive charge¹⁵ associated with at least 50% of the I^{128} atoms is an important factor in the reaction.

We have been interested in determining qualitatively the mechanism of the reaction of I^{128} with CH_4 . To do this, we have investigated the manner in which the reaction to produce organic I^{128} is moderated by varying amounts of inert-gas and molecular additives.

Effect of Inert-Gas Additives

Summarized in Table VIII are the observed extents of production of organically bound I^{128} for various methane-inert gas reaction systems. Data for I^{131} pickup are also included. These mixtures contained four substances: methane, inert gas, 0.5 mm. CH_3I , and 0.1 mm. I_2 scavenger.

In order to interpret properly the relative effects of the additives, it is necessary to correct these data of Table VIII for (a) the 1.1% failure to bond rupture of CH_3I and (b) any radiation induced reactions.

Radiation induced reactions. Mixtures containing I_2 tagged with I^{131} were also irradiated; the percent I^{131} appearing in organic combination is listed in Table I. These data are also depicted in Fig. 11. Negligible I^{131} pickup was found in I_2-CH_4 systems which did not contain an inert-gas additive.

In order to avoid any possible thermal or photochemical exchange reaction between the I_2-131 and CH_3I , all samples were prepared in a minimum of light and, if neutron irradiation was not immediately feasible, stored at $0^\circ C$ in the dark. This technique

Table VIII - Percent I^{128} (and I^{131}) Stabilized in Organic Combination in Various Gaseous Mixtures^a

Additive	Pressure CH ₄ - mm	Pressure Additive mm	Mole Fraction Additive ^b	Percent I^{128} as Organic ^c	Percent I^{131} as Organic ^d
Neon	594	76	0.113(11)	52.9	
	489	159	0.245(8)	53.1 52.2	
	308	128	0.294(24)	53.3 52.8	2.6 2.2
	362	231	0.390(45)	50.0 54.0	
	205	133	0.394(32)	50.1	
	205	129	9.386(32)	50.1	
Argon	400	189	0.321(27)	54.3 54.5	3.8 3.9
	295	235	0.443(31)	52.2 52.0	3.0 2.0
	109	410	0.765(59)	45.4 47.4	
	50	341	0.872(67)		1.0 1.5
Krypton	595	80	0.119(2)	53.8 53.5	
	483	106	0.180(3)	52.4	5.1
	320	120	0.273(3)	49.5 48.5	
	432	236	0.353(3)	50.5 51.8	6.2 7.3
	194	141	0.421(1)	45.6 45.0	

Table VIII (Cont.)

Additive	Pressure CH ₄ - mm	Pressure Additive mm	Mole Fraction Additive ^b	Percent I ¹²⁸ as Organic ^c	Percent I ¹³¹ as Organic ^d
Krypton	143	412	0.742(4)	49.3	8.8
				49.0	9.1
	43	456	0.914(3)	48.0	10.8
Xenon	615	40	0.061(2)	50.8	
				50.5	
	563	61	0.098(4)	48.3	2.3
				47.3	2.5
	554	101	0.154(2)	45.2	
				46.5	
	489	179	0.268(2)	39.6	
				39.8	
	251	307	0.552(4)	31.6	7.7
				29.4	8.0
	179	331	0.649(4)	30.5	
				29.2	
	72	447	0.865(5)	31.0	16.0
				30.4	14.0
	60	454	0.883(5)	29.2	
				29.3	
	23	515	0.957(5)	24.1	
				24.5	

^a All samples contained 0.1 ± 0.01 mm I₂ and 0.5 ± 0.1 mm CH₃I and were irradiated for 7 sec.

^b Calculated assuming additive pressures. Uncertainty in last figure or figures (given in parenthesis) is based on estimates of determining individual pressures.

^c An uncertainty of ± 0.5 was associated with the positioning of the 25.0 min slope through the decay data.

^d An uncertainty of ± 1.5 was associated with the decay data and possible pre-irradiation I₂ - CH₃I exchange.

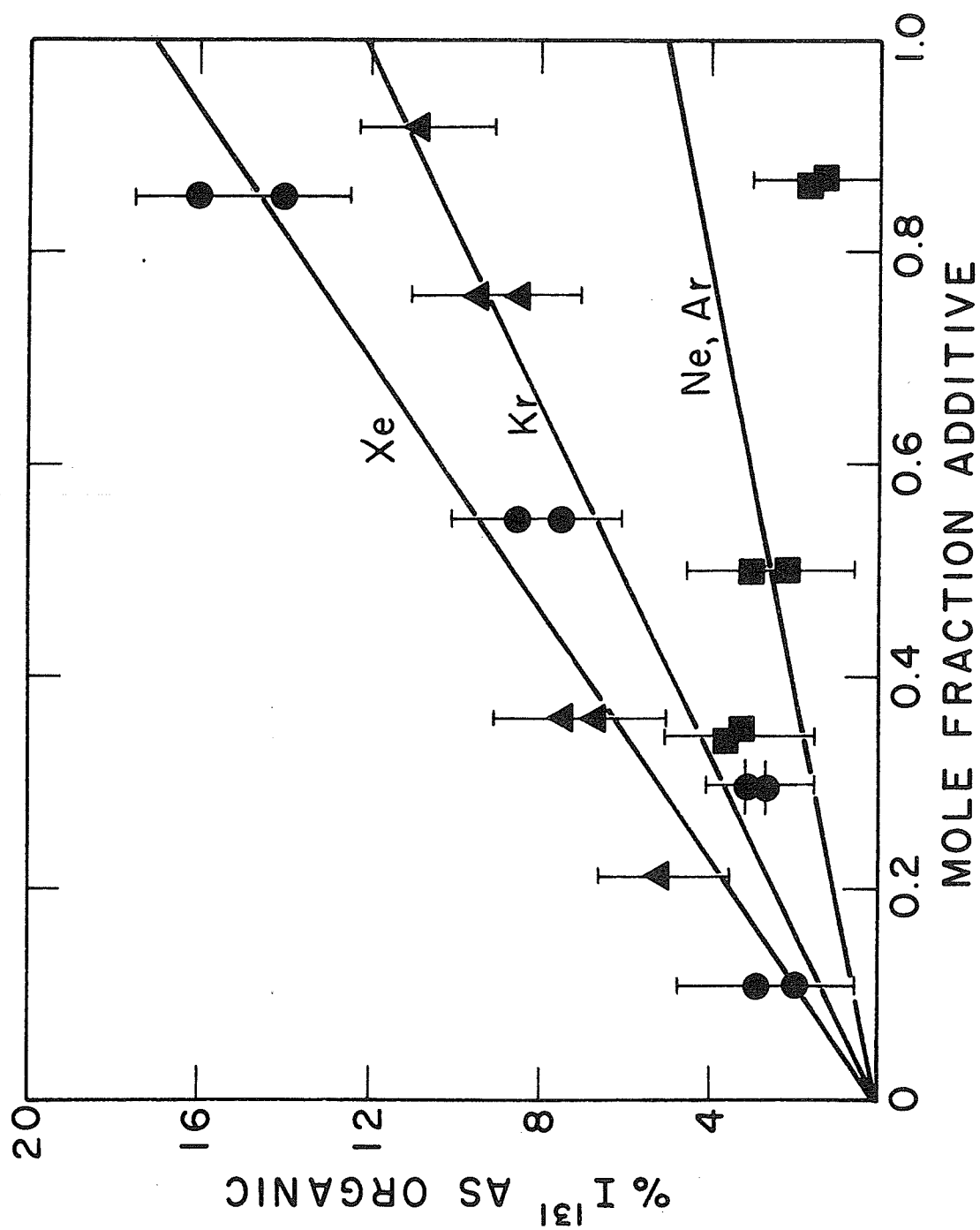


Fig. 11 - Reactor-radiation induced pickup of I^{131} in CH_4 - inert gas mixtures containing CH_3I and I_2 - ^{131}I . Xenon, ● ; krypton, ▲ ; argon, ■ ; neon, ●-.

resulted in a pre-irradiation I^{131} organic pickup of only 0 - 1.5%.

The relative extents of radiation induced reactions for these inert gases are about 17:12:5 which is approximately in the same ratio as the number of electrons in the inert gases. This is as would be expected since the average energy of the gamma rays in a nuclear reactor is of the order of 2 Mev and the interaction of such gamma rays with matter proceeds mainly via Compton scattering, the interaction probability being related directly to the first power of the atomic number of the material.

If a sample contained I^{131} , the observed percent organic I^{131} was subtracted from the organic I^{128} yield. For those samples not containing I^{131} , the correction for radiation induced reactions was determined in terms of the straight-line plots of Fig. 11. These I^{128} data of Table VIII, corrected for failure to bond rupture and radiation induced reactions, are depicted in Fig. 12.

Maximum extent of reaction. Extrapolations of the various data given in Tables VIII and IX to zero mole-fraction of additive indicate that $54.4 \pm 0.5\%$ of the I^{128} reacts with methane to become stabilized in organic combination.

On the basis of previous gas chromatographic analyses⁴, it is known that CH_3I^{128} is the major organic product. The only other observable organic product was CH_2II^{128} , present to the extent of only about 1%.

Discussion

If the CH_3I^{128} is formed only as a result of a hot reaction, then a large excess of an inert gas should be capable of suppressing completely the formation of CH_3I^{128} . As seen in Fig. 12, the inert gases only partially suppress the reaction. Apparently, then, only a fraction of the CH_3I^{128} is formed via a hot reaction, the remainder being formed via thermal processes. It should be noted that xenon reduces the CH_3I^{128} yield to $11 \pm 2\%$, whereas other inert gases reduce this yield to only about $36 \pm 2\%$. The assumption that the reduction to 36% is a result mainly of a hot

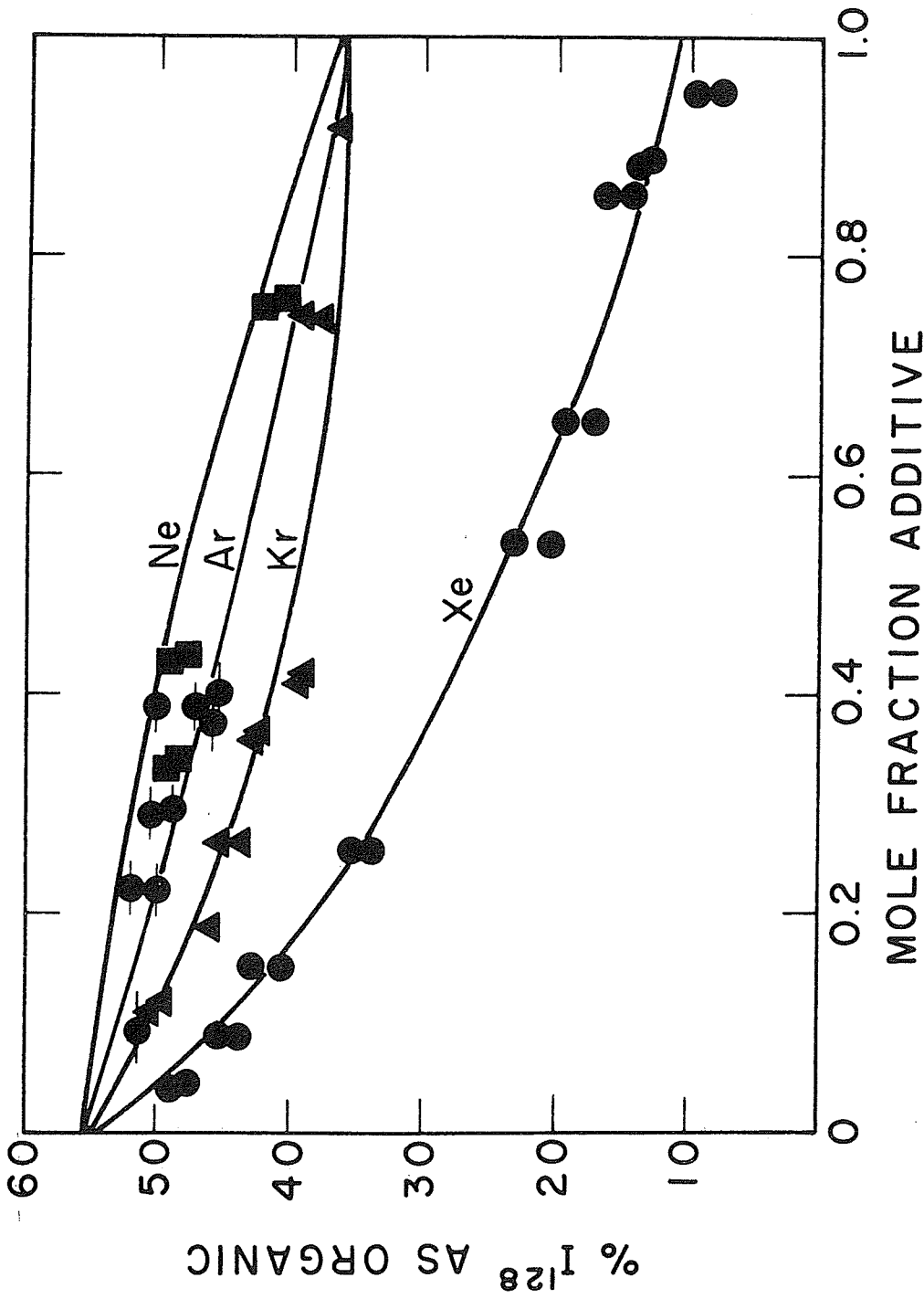


Fig. 12 - Percent I^{128} formed as organic activity in CH_4 - inert gas mixtures containing CH_3I and I_2 . Moderator symbols are listed in caption for Fig. 11. The solid curves are calculated.

reaction is justified by the mathematical analysis given in the next section.

The fact that xenon reduces the extent of formation of $\text{CH}_3\text{I}^{128}$ by an additional $25 \pm 3\%$ must be due to a unique ability of xenon to neutralize or quench excited I^{128} ions or atoms. Inert gases, however, are not effective quenching agents¹¹. Therefore, this additional moderation by xenon must be due to a charge-transfer process. For xenon alone to exhibit moderation by charge transfer requires that the energy defect of the reaction approach zero more closely than that for charge transfer with the other inert gases.

The first four excited states of I^+ and their excitation energies are as follows: ($^3\text{P}_0$) 0.800, ($^3\text{P}_1$) 0.879, ($^1\text{D}_2$) 1.702, ($^1\text{S}_2$) 4.044 ev. It is unlikely that excited ionic states higher than the $^1\text{D}_2$ will exist in the methane environment. The ionization potential of CH_4 is 12.99 ev. For the process $\text{I}^+(^1\text{D}_2) + \text{CH}_4 \rightarrow \text{I} + \text{CH}_4^+$ to occur, the relative energies of the reacting species must be much greater than that supplied by the (n, γ) activation¹². However, charge transfer between CH_4 and I^+ in the $^1\text{S}_2$ or higher states are exothermic and very probable since the excess energy (the energy defect) is assimilated by the various internal degrees of freedom of the methane ion.

The ionization potential of an iodine atom is 10.454 ev and that of xenon is 12.127 ev. Thus, the process $\text{I}^+(^1\text{D}_2) + \text{Xe} \rightarrow \text{I} + \text{Xe}^+$ is exothermic by 0.029 ev. For this near-resonance charge-transfer process, the cross-section will be maximum for relative energies of about 2 ev and slowly decrease for energies greater than 2 ev¹⁴. The smallest energy defect for the possible charge-transfer processes involving the other inert gases is 1.840 ev endothermic for the $\text{I}^+(^1\text{D}_2) + \text{Kr}$ reaction. Hence, these processes involving Kr, Ar, or Ne charge-transfer with I^+ ions in energy states of $^1\text{D}_2$ or less have an extremely small probability of occurrence.

Using the notation of Estrup and Wolfgang, we have calculated α values and f values for the species involved in the reaction. It is important to emphasize that attempts to fit directly the data of Fig. 12 to this kinetic theory were unsuccessful. If,

however, we assume that the maximum inert-gas kinetic-energy moderation is $54.4 - 36 = 18.4\%$, then we find that the theory serves to describe the observed effects.

Neon, argon, krypton. Thirty-six percent was subtracted from the individual values for the Ne, Ar, and Kr samples. For essentially pure methane, $f/\alpha = 4.29$; thus, $(\alpha/f) \cdot (\text{fraction of } I^{128} \text{ as organic}) = 0.0428$. Figure 13 is a plot of the experimental data corresponding to Eq. (32). The best visual straight line drawn through the data and ending at the point (0.0428, 4.29) has a slope $-K = -0.004 \pm 0.003$ and an intercept $I = 0.06 \pm 0.01$. It is interesting to note that, within the limits of uncertainty, these values correspond to those found for the $\text{Br}^{80} + \text{CH}_4$ reaction. The solid curves of Fig. 12 for Ne, Ar, and Kr were calculated using these values of K and I.

Xenon. As stated earlier, the xenon data are not described by the kinetic theory. A lack of agreement still exists even after subtracting 11% from each experimental result. It was suggested in the previous section that xenon could be a more effective moderator since it could easily undergo charge transfer with $I^+(^1D_2)$. To determine the moderation via the charge-transfer process, we subtracted from the original data: (1) the 1.1% CH_3I failure to bond rupture, (2) the 11% organic I^{128} which is not effected by xenon, and (3) the expected kinetic-energy moderation by xenon. This last factor varied from zero to 18.4% and was calculated in terms of Eq. (32) using the slope and intercept determined from Fig. 13 above. Depicted in Fig. 14 is the percent organic I^{128} remaining after correcting for these three effects.

Let us assume that this remaining extent of reaction of I^{128} with methane to produce organically bound I^{128} , R, depends on the probability, P, that the I^{128} "collides" with CH_4 . Thus, $R = 25P$. The probability will depend on (1) the mole fraction of methane, $(1 - N)$, where N is the mole fraction of additive and (2) the relative cross-sections, C, for the two-types of interactions; $C = \sigma(I^+(^1D_2) + \text{Xe charge exchange}) / \sigma(I^+(^1D_2) + \text{CH}_4 \text{ to yield } \text{CH}_3I^{128})$. Using these definitions, $C = \{ (25 - R)(1 - N) \} / RN$.

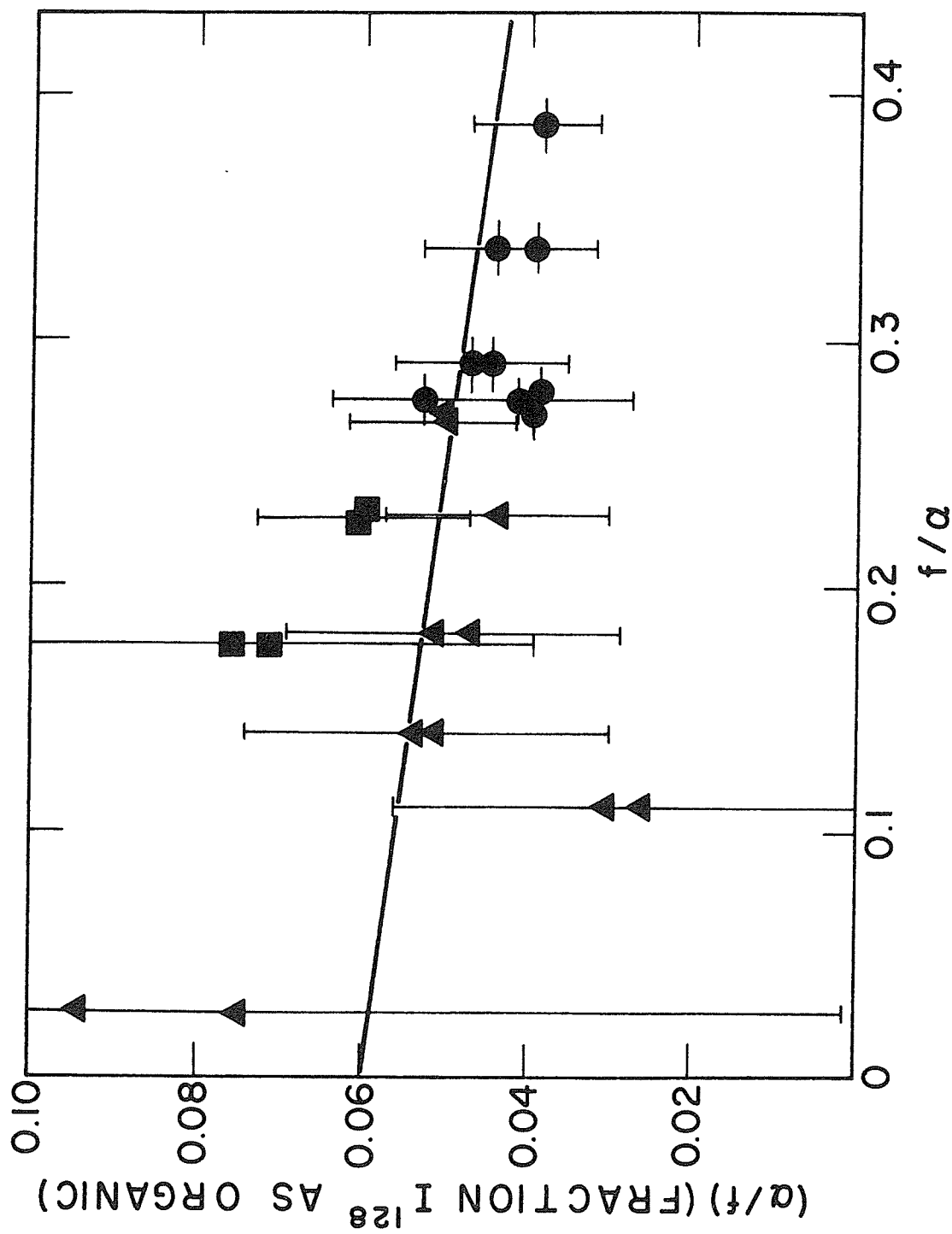


Fig. 13 - Plot corresponding to Eq. 32. Moderator symbols are listed in captions for Fig. 11.

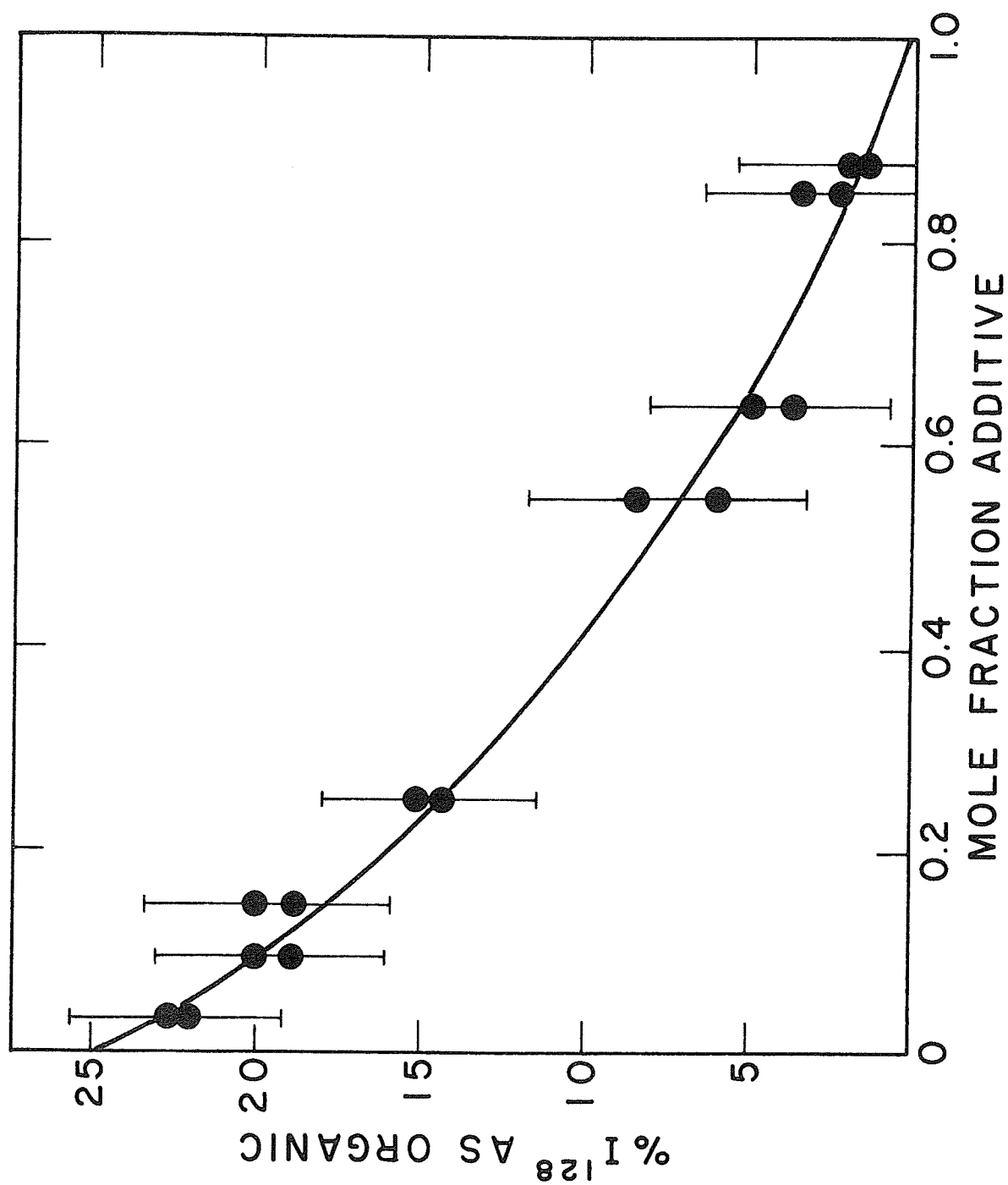


Fig. 14 - Effect of xenon in moderating the reaction $I^+(^1D_2) + CH_4 \rightarrow CH_3I^+ + H$.
The solid curve is calculated.

The value of C calculated from the data of Fig. 14 is 2.2 ± 0.6 . Considering the various subtractions and uncertainties, it is somewhat fortuitous that the calculated C values are in reasonable agreement. The solid curve of Fig. 14 was calculated using this value of C .

It is reasonable to expect the excited iodine ions to react prior to becoming deactivated by fluorescence. The iodine ions would have undergone of the order of 1000 collisions in the 10^{-8} to 10^{-7} sec. associated with fluorescent deactivation. Only in systems containing a large excess of inert gas would there be a possibility of fluorescent deactivation. This could be the reason that the last xenon data of Fig. 12 are somewhat low.

Reaction Processes

On the basis of the previous discussions, we conclude that of the $54.4 \pm 0.5\%$ I^{128} found as organic:

$18.4 \pm 2\%$ is formed via a hot reaction. The experimental evidence, however, is insufficient to conclude whether the hot I^{128} species is an ion or an atom.

$25 \pm 3\%$ is formed as a result of the $I^+(^1D_2) + CH_4$ reaction. Considering the energy requirements, if the reaction is a simple hydrogen displacement, then the reaction must be $I^+(^1D_2) + CH_4 \rightarrow CH_3I^+ + H$.

$11 \pm 2\%$ is formed as a result of the reaction of I^{128} ions (or excited atoms). Either 3P_2 , 3P_1 , or 3P_0 I^+ ions are involved since, as stated above, ions in energy states greater than the 1D_2 would not exist in the methane environment. If the ionic reaction taking place involves hydrogen displacement then, considering the energy available, the reaction must also be $I^+ + CH_4 \rightarrow CH_3I^+ + H$.

The manner in which the CH_3I^+ gains an electron is not known. It is difficult to accept electron capture as the process. The 9.54 ev exothermicity would most probably be partially dissipated in the form of the internal energy of the molecule and thus probably result in C-I bond rupture. If, instead, C-H bond rupture

occurred, then, because of the presence of I_2 in the reaction system, CH_2I_2 should be a major product. Gas chromatographic analysis⁴ indicated that only a small amount of CH_2I_2 was formed. However, because of the presence of CH_3I and I_2 in the reaction mixture, neutralization of the CH_3I^+ probably takes place via charge transfer.

Effect of Molecular Additives

Contained in Table IX are data of the percent I^{128} found as organic for various mixtures of molecular additive, methane, 1-2 mm CH_3I , and 0.1 mm I_2 . Table X is a summary of the percent I^{128} stabilized in organic combination in various non-methane systems where the additive molecule was in large excess.

The raw data of Table IX were corrected for (a) the extent of failure to bond-rupture of the alkyl-iodide, (b) any gamma-radiation induced formation of organic I^{128} compounds, and (c) the extent to which I^{128} is organically bound as a result of reaction with the additive.

The percent failure to bond-rupture used in correcting the data are: CH_3I - 1.1, $n-C_3H_7I$ - 0.7, and CF_3I - 0.1%.

The maximum extents of reaction with the additives to produce organic I^{128} are, correcting for any failure to bond-rupture: CF_4 - 3.4, CH_2F_2 - 2.2, C_2F_6 - 7.8, C_6H_6 - 1.6, $n-C_3H_7I$ - 0.6, and CH_3I - 0.2%. The product of the mole-fraction of the additive multiplied by the extent of reaction with "pure" additive, as given above, was subtracted from the raw data of Table IX.

Table IX

Organic Yields of Iodine-128 with Methane at
Various Mole Fractions of the Following Additives

Additive	Pressure CH ₄ (mm)	Pressure Additive (mm)	Mole Fraction Additive	Uncorrected % I ¹²⁸ as Organic	Corrected % I ¹²⁸ as Organic ^a
O ₂	574.0	80.0	0.122(11)	53.5	51.8
	574.0	87.0	0.132(6)	53.5	51.7
	459.0	180.0	0.282(19)	53.0	50.5
	459.0	192.0	0.295(13)	50.8	48.2
	35.0	482.0	0.932(7)	40.5	34.7
				43.0	37.2
N ₂	608.0	59.0	0.089(9)	49.6	48.4
	608.0	65.0	0.097(6)	53.6	52.0
	529.0	132.0	0.200(16)	51.1	49.0
	529.0	148.0	0.219(9)	54.9	52.7
	411.0	207.0	0.335(26)	54.5	51.7
	35.0	329.0	0.890(12)	48.2	42.6
				46.8	41.2
CF ₄	577.0	93.0	0.139(2)	52.7	51.1
				52.7	51.1
	445.0	249.0	0.359(2)	50.0	47.4
				50.1	47.5
	247.0	429.0	0.635(3)	47.3	43.5
				47.6	43.8
	67.0	640.0	0.905(4)	42.6	37.4
				42.8	37.6
	35.0	653.0	0.950(3)	42.2	36.8
				42.7	37.3
CH ₂ F ₂	545.0	146.0	0.211(2)	45.3	43.4
				46.6	44.7
	282.0	168.0	0.373(3)	42.7	40.2
				44.1	41.6

Table IX (Cont.)

Additive	Pressure CH ₄ (mm)	Pressure Additive (mm)	Mole Fraction Additive	Uncorrected % I ¹²⁸ as Organic	Corrected % I ¹²⁸ as Organic ^a
CH ₂ F ₂	284.0	283.0	0.499(3)	37.1	34.5
	229.0	450.0	0.663(3)	31.0 31.5	27.4 27.9
C ₂ F ₆	590.0	92.0	0.135(2)	48.8 49.2	44.8 45.2
	367.0	188.0	0.339(2)	39.7 44.0	31.1 35.5
	389.0	311.0	0.444(4)	42.0	31.1
	399.0	331.0	0.453(2)	42.0 44.3	30.8 33.2
	171.0	287.0	0.627(4)	39.5	24.2
	150.0	520.0	0.776(3)	40.2 41.4	21.4 22.7
	14.0	649.0	0.979(4)	37.2 37.3	13.2 13.3
	679.0	9.0	0.013(1)	52.9 51.8	51.8 50.7
	674.0	13.0	0.019(1)	49.4 51.0	48.3 49.9
NO	652.0	16.0	0.024(1)	47.2 51.6	46.1 50.5
	454.0	38.0	0.077(2)	42.6 43.0	41.5 41.9
	373.0	44.0	0.106(2)	39.6 39.3	38.5 38.2
	562.0	112.0	0.166(1)	35.5 36.8	34.4 35.7
	457.0	132.0	0.224(2)	34.1 31.1	33.0 30.0

Table IX (Cont.)

Additive	Pressure CH ₄ (mm)	Pressure Additive (mm)	Mole Fraction Additive	Uncorrected % I ¹²⁸ as Organic	Corrected % I ¹²⁸ as Organic ^a
NO	289.0	161.0	0.357(2)	26.2	25.1
				25.1	24.0
	149.0	561.0	0.790(1)	9.2	8.1
				9.9	8.8
CH ₃ I	721.0	1.0	0.001(1)	54.8	53.7
	710.0	22.0	0.003(1)	55.0	53.9
				53.4	52.3
	665.0	3.0	0.005(1)	54.2	53.1
				53.9	52.8
	659.0	7.0	0.011(1)	47.1	46.0
				47.8	46.7
	558.0	10.0	0.018(1)	42.2	41.1
				42.3	41.2
	532.0	12.0	0.022(1)	39.2	38.1
				40.6	39.5
	460.0	11.0	0.023(2)	38.5	37.4
				37.9	36.8
	342.0	12.0	0.034(2)	33.5	32.4
				33.7	32.6
	186.0	12.0	0.061(4)	24.5	23.4
	233.0	22.0	0.086(3)	17.6	16.5
				17.6	16.5
	131.0	22.0	0.144(5)	11.7	10.6
	111.0	34.0	0.234(6)	7.4	6.3
				5.9	4.8
	197.0	128.0	0.417(5)	4.2	3.1
				3.9	2.8
	132.0	163.0	0.553(5)	2.9	1.8
				2.5	1.4

Table IX (Cont.)

Additive	Pressure CH ₄ (mm)	Pressure Additive (mm)	Mole Fraction Additive	Uncorrected % I ¹²⁸ as Organic	Corrected % I ¹²⁸ as Organic ^a
C ₃ H ₇ I	684.0	7.0	0.010(1)	44.7	43.6
				44.8	43.7
	678.0	15.0	0.022(1)	37.4	36.3
				35.2	34.1
	482.0	28.0	0.055(1)	28.9	27.8
				27.3	26.2
	288.0	21.0	0.068(2)	20.1	19.0
				18.6	17.5
	187.0	22.0	0.105(1)	15.9	14.8
				11.4	10.3
	181.0	25.0	0.121(4)	14.9	13.8
				11.8	10.7
CF ₃ I	620.0	16.0	0.025(1)	35.4	34.3
				33.7	32.6
	178.0	42.0	0.191(4)	6.6	5.5
				5.9	4.8
C ₆ H ₆	646.0	10.0	0.015(1)	46.4	45.3
				48.4	47.3
	659.0	15.0	0.022(1)	37.7	36.6
				37.6	36.5
	675.0	27.0	0.039(1)	31.4	30.3
				32.4	31.3
	155.0	27.0	0.148(2)	9.7	8.6
				9.2	8.1

^a Refer to text for method of correction.

Table X

Percent I^{128} Stabilized in Organic Combination in
Various Gaseous Mixtures of an Iodide and Additive

Iodide	Additive	Total Pressure	Mole Fraction Additive	% I^{128} as Organic	
$CH_3I(I_2)$	CF_4	622	0.994	4.6(4)	4.4(4)
$CH_3I(I_2)$	CH_2F_2	650	0.985	3.5(1)	3.0(1)
		710	0.976	3.4(1)	2.9(1)
$CH_3I(I_2)$	C_2F_6	623	0.997	8.9(2)	8.8(7)
I_2	C_6H_6	31	0.997	1.2(1)	1.5(1)
$CH_3I(I_2)$	--	28		1.4(1)	
		18		1.3(1)	
		18		1.2(1)	
$n-C_3H_7I(I_2)$	--	19		1.3(1)	
$CF_3I(I_2)$	--	44	0.998	1.1(1)	1.2(1)

A similar calculation was used in correcting for gamma-radiation induced reactions. To do this, the extent of radiation-induced reaction at unit mole fraction was determined. The extent of radiation-induced reactions then was assumed to be equal to the product of the mole-fraction of the additive times this maximum value. For O_2 and N_2 this maximum value was assumed equal to that of Ne-Ar (5%). For C_2F_6 it was found experimentally to be 17%, for CF_4 , 3%. The value for CH_2F_2 was assumed to be less than that of CF_4 and chosen as 2%.

The percent organic I^{128} corrected for these effects is also given in Table IX.

N_2 , O_2 , and CF_4 Additives

Depicted in Fig. 15 are the corrected data for N_2 , O_2 , and CF_4 moderation. These data appear to extrapolate to 36% suggesting that these additives moderate the $I^{128} + CH_4$ reaction only by removing I^{128} excess kinetic energy. The solid curves were calculated according to Eq. (32) using values of I and K calculated from the inert-gas data (Fig. 13). Fig. 15 suggests that N_2 , O_2 , and CF_4 are inefficient in quenching excited I^{128} ions or atoms.

CH_2F_2 and C_2F_6 Additives

Depicted in Fig. 16 are the data for moderation by CH_2F_2 and C_2F_6 . These data appear to extrapolate to a value of about 11% suggesting that they not only remove excess kinetic energy but also interact with $I^+(\hat{1}D_2)$ ions.

The broken curves of Fig. 16 were calculated according to Eq. 32. The inhibition in excess of kinetic energy moderation was determined by subtracting from the data the value calculated via Eq. 32. Subtracting 11% from this value there are obtained data which should be analogous to that of Fig. 14. For these remaining data we calculated "C" values in a manner indicated on

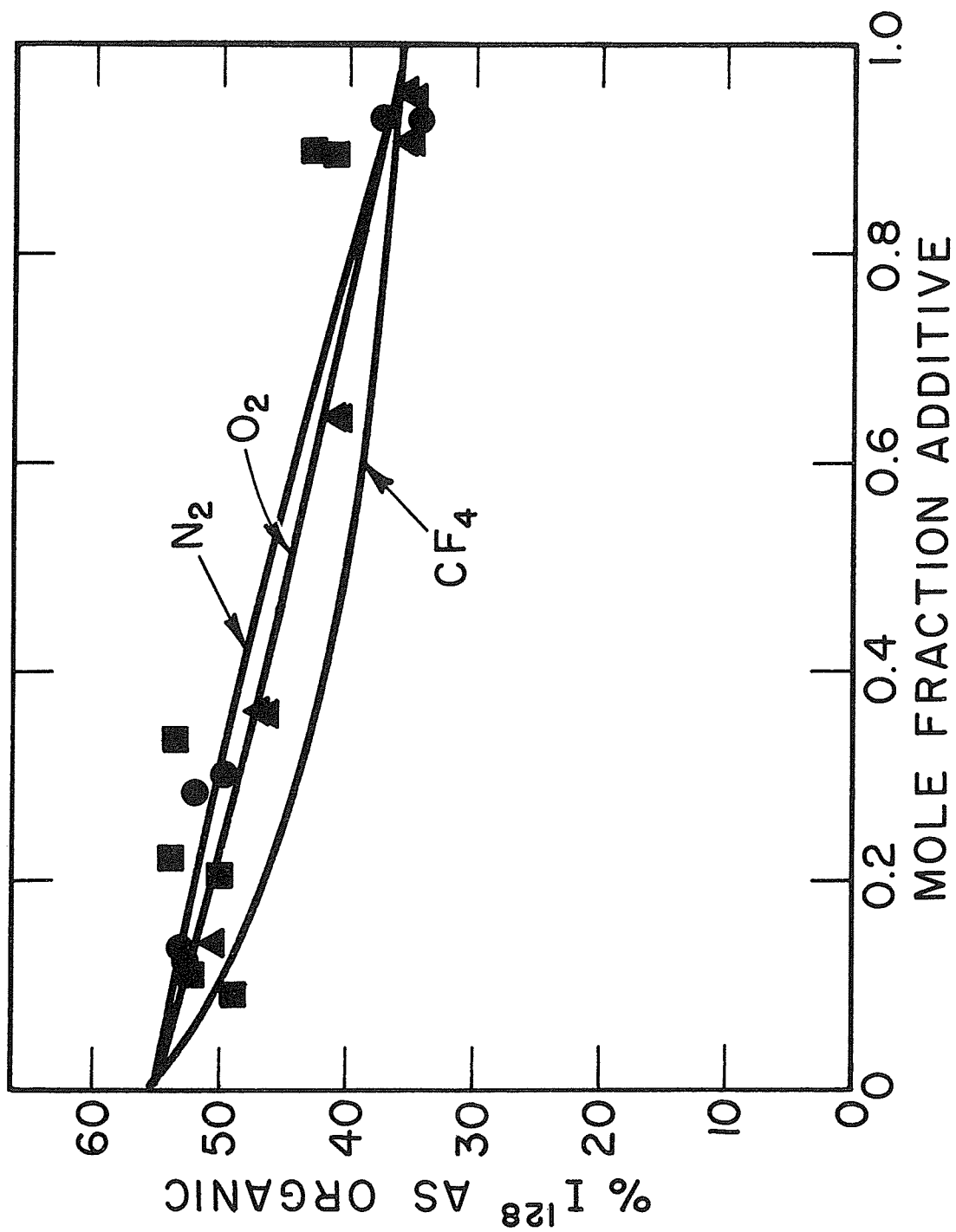


Fig. 15 - Effect of molecular additives on the reaction of gaseous CH_4 with I^{128} .
Moderators: O_2 , ● ; N_2 , ■ ; CF_4 , ▲ .

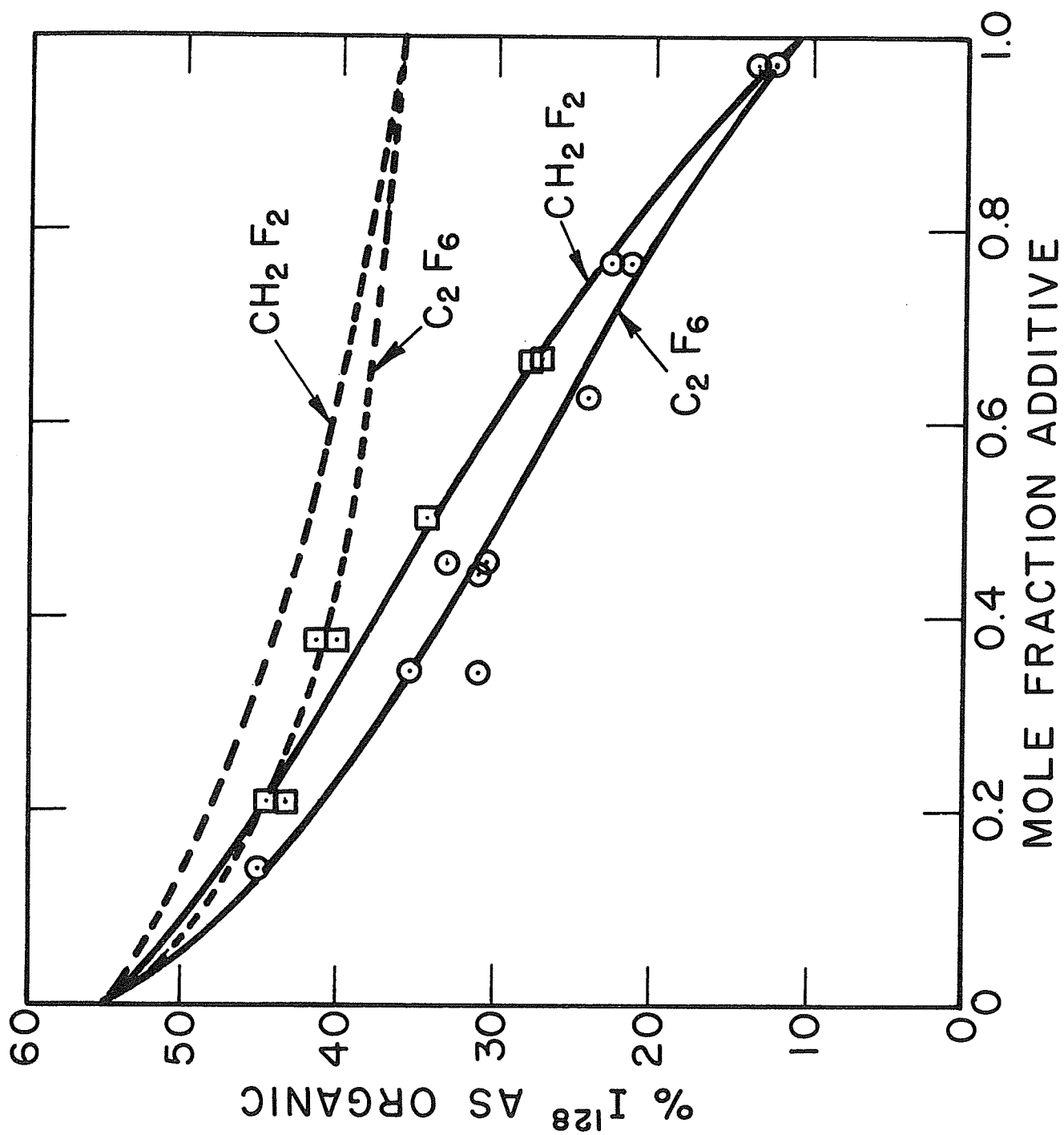


Fig. 16 - Effect of molecular additives on the reaction of gaseous CH_4 with I^{128} .
Moderators: CH_2F_2 , \square ; C_2F_6 , \circ .

page 58. These values were 0.50 for CH_2F_2 and 0.72 for C_2F_6 .

Apparently, these two compounds interact with $\text{I}^+(\text{}^1\text{D}_2)$ ions with different efficiencies. The ionization potential of CH_2F_2 is most probably greater than that of CH_4 (12.99 ev). Since the $\text{I}^+(\text{}^1\text{D}_2)$ ionization potential is $10.45 + 1.70 = 12.15$ ev, charge transfer between CH_2F_2 and $\text{I}^+(\text{}^1\text{D}_2)$ would be highly unlikely. The ionization potential of C_2F_6 , however, is probably greater than 11.67 ev. If it is less than 12.15 ev charge transfer is highly probable.

Reaction with the additive could result in the observed inhibition of the $\text{I}^{128} + \text{CH}_4$ reaction. Reaction of I^{128} with C_2F_6 to yield organic or inorganic I^{128} requires more energy than associated with $\text{I}^+(\text{}^1\text{D}_2)$ ions. However, reaction of thermal $\text{I}^+(\text{}^1\text{D}_2)$ ions with CH_2F_2 to yield $\text{CHF}_2^+ + \text{HI}$ is possible; lower state I^+ ions do not possess enough energy. Thus, it appears that inhibition of the $\text{I}^{128} + \text{CH}_4$ by CH_2F_2 is a result of kinetic energy moderation (18%) and reaction with CH_2F_2 (25%). The additional 25% inhibition by C_2F_6 most probably is due to charge transfer thus limiting the ionization potential of C_2F_6 to 11.67 - 12.15 ev.

NO, CH_3I , n- $\text{C}_3\text{H}_7\text{I}$, CF_3I , and C_6H_6 Additives

These additives all possess ionization potentials less than that of an iodine atom. The inhibition exhibited by these additives (Fig. 17) is much greater than that of O_2 , N_2 , CF_4 , CH_2F_2 , and C_2F_6 . It would appear as though these additives of low ionization potential inhibit principally by charge neutralization. However, the large inhibition resulting from CH_3I , n- $\text{C}_3\text{H}_7\text{I}$, CF_3I , and C_6H_6 may be due to ion-molecule reactions. For example, the reaction: $\text{I}^+ + \text{CH}_3\text{I} \rightarrow \text{CH}_3 + \text{I}_2^+$ is possible.

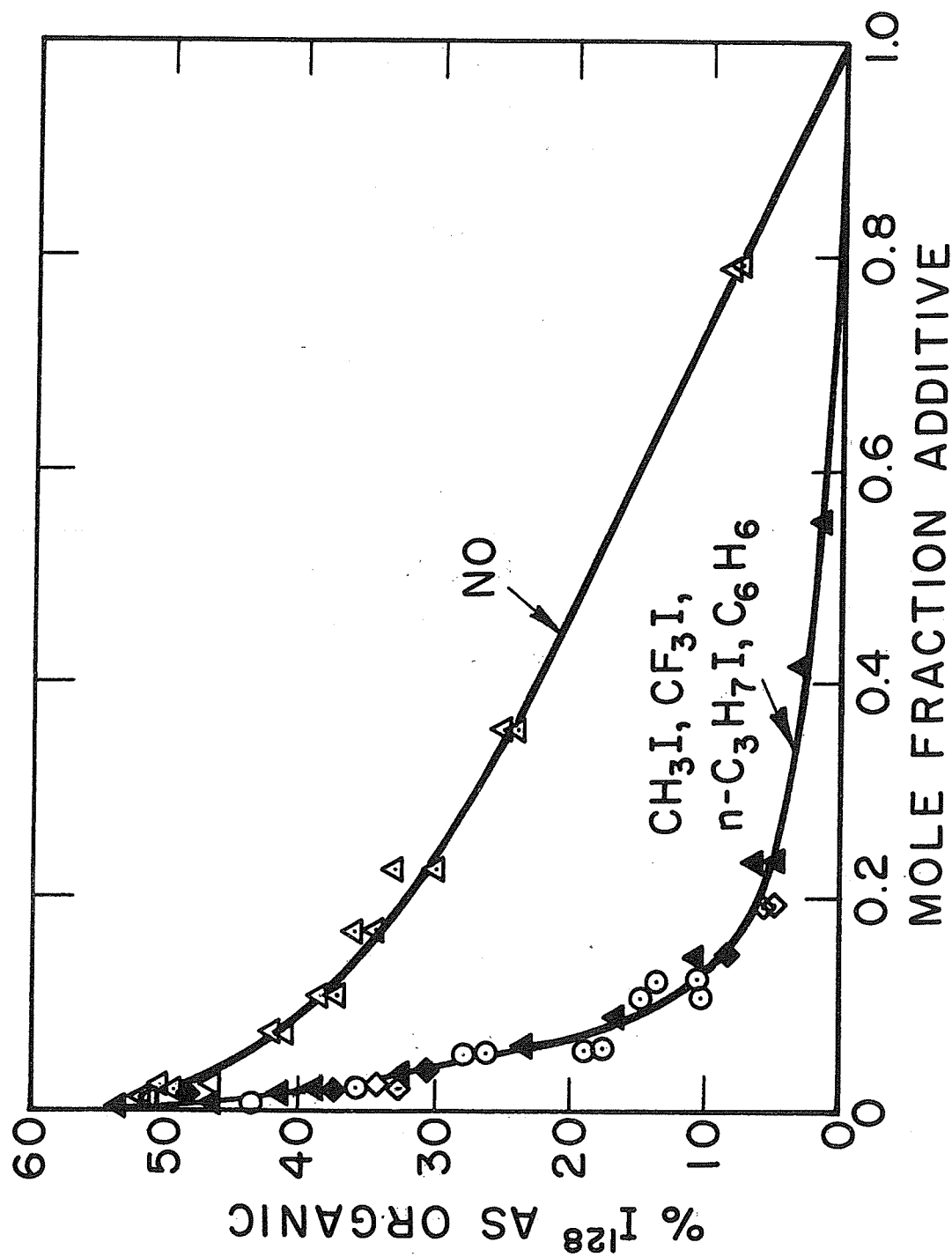


Fig. 17 - Effect of molecular additives on the reaction of gaseous CH_4 with I^{128} .
Moderators: NO, Δ ; CH_3I , \blacktriangle ; CF_3I , \diamond ; C_6H_6 , \blacklozenge ; $n-C_3H_7I$, \odot .

VIII. WORK IN PROGRESS

The work in progress includes:

1. Studies of the reactions of Cl^{38} produced by the $\text{Cl}^{37}(\text{n},\gamma)\text{Cl}^{38}$ process.
2. Gas and liquid phase studies of similar systems, particularly iodine + chlorocarbon mixtures.
3. Gas-chromatographic analysis of reaction products.
4. Effect of additives on such reactions as $\text{I}^{128} + \text{CHF}_3$.
5. Studies of the effects of cobalt-60 gamma radiation on halogen-methane-additive systems.
6. Studies of the failure to bond-rupture of chlorocarbons.
7. Theoretical analysis of high energy reaction mechanisms.
8. Effect of additives on the gas phase reaction: $\text{Br}^{80} + \text{CH}_4$ where activation is by isomeric transition.

IX. PERSONNEL AND PUBLICATIONS

A. Personnel

1. Principal Investigator

Adon A. Gordus

2. Graduate Students (1/2 time)

Edward P. Rack

Ruth (Chi-hua) Hsiung

Harry (Hsièn-chih) Hsiung

Navanitray C. Kothary (as of Jan. 1, 1961)

Jack Brillhart (Summer, 1960)

Bernard Spielvogel (Summer, 1960)

3. Undergraduate Assistants (part-time, hourly)

William Rado

Alan Frew

Richard Siemon

Wolf Blatter (as of Sept. 1, 1960)

Martin Cooper (Summer, 1960)

Ronald Fine (Summer, 1960)

B. Publications

1. "A Closed General Solution of the Probability Distribution Function for Three Dimensional Random Walk Processes" by C. Hsiung, H. Hsiung, and A. A. Gordus, J. Chem. Phys., 34, 535-546 (1961).
2. "Effect of Moderators on the (n, γ) Activated Reaction of Br⁸⁰ with CH₄" by E. P. Rack and A. A. Gordus, to appear in April or May, 1961, issue of the Journal of Physical Chemistry.
3. "Effect of Inert-Gas Moderators on the (n, γ) Activated Reaction of I¹²⁸ with CH₄" by E. P. Rack and A. A. Gordus, to appear in June, 1961, issue of the Journal of Chemical Physics.
4. "Effect of Molecular Additives on the (n, γ) Activated Reaction of I¹²⁸ with CH₄" by E. P. Rack and A. A. Gordus, submitted for publication.

5. "Vibrational and Rotational Excitation Resulting from Momentum Transfer" by C. Hsiung and A. A. Gordus, submitted for publication.
6. "Gamma-Ray Momentum Transfer: Carbon-Halogen Failure to Bond-Rupture Following (n,γ) Activation" by A. A. Gordus, submitted for publication.

C. Talks

A series of talks were given before local groups which included the U. of Michigan chapter of the Am. Soc. of Met. Eng. and the Flint subdivision of the Detroit section of the American Chemical Society. In addition, two papers were presented at the International Symposium on the Chemical Effects of Nuclear Transformations which was sponsored by the IAEA and held in Prague, October 24-27, 1960. These papers were:

CENT/49 - Gamma Recoil Energy Distributions

CENT/59 - Hot Ion-Molecule Gas Phase Reactions of (n,γ) Activated I^{128} , Br^{80} , and Cl^{38} with Hydrocarbons and Alkyl-Halides.

X. REFERENCES

1. C. Hsiung, H. Hsiung, and A. A. Gordus, J. Chem. Phys., 34, 535 (1961).
2. See, for example, R. R. Edwards and T. H. Davies, Nucleonics, 2, 44 (1948).
3. H. Suess, Z. Physik Chem., B45, 312 (1940).
4. A. A. Gordus and J. E. Willard, J. Am. Chem. Soc.,
5. H. Steinwedel and J. H. D. Jensen, J. Naturforsch. A2, 195 (1947).
6. K. Svoboda, Zhur. Neorg. Khim, 3, 187 (1958); U. S. Atomic Energy Comm. Nuclear Sci. Abstr. 13, 10954 (1959).
7. M. Wolfsberg, J. Chem. Phys., 24, 24 (1956).
8. R. L. Wolfgang, R. C. Anderson, and R. W. Dódson, 24, 16 (1956).
9. P. J. Estrup and R. Wolfgang, J. Am. Chem. Soc., 82, 2665 (1960).
10. J. B. Evans, J. E. Quinlan, M. C. Sauer, Jr., and J. E. Willard, J. Phys. Chem., 62, 1351 (1958).
11. K. J. Laidler, The Chemical Kinetics of Excited States (Oxford University Press, Oxford, 1955), p. 105.
12. E. F. Gurnee and J. L. Magee, J. Chem. Phys., 26, 542 (1957).
13. J. F. Hornig, G. Levey, and J. E. Willard, J. Chem. Phys., 20, 1556 (1952).
14. G. Levey and J. E. Willard, J. Chem. Phys., 25, 904 (1956).
15. S. Wexler and H. Davies, J. Chem. Phys., 20, 1688 (1952).